UNIVERSIDADE FEDERAL DE PERNAMBUCO
CENTRO DE TECNOLOGIAS E GEOCIÊNCIAS
DEPARTAMENTO DE GEOLOGIA
PROGRAMA DE PÓS-GRADUAÇÃO EM GEOCIÊNCIAS

DANIELLE CRUZ DA SILVA

# ORIGEM E CARACTERIZAÇÃO DO QUARTZO AZUL EM METARRIOLITOS DO GRUPO RIO DOS REMÉDIOS, PARAMIRIM (BA)

Recife
2023

DANIELLE CRUZ DA SILVA

# ORIGEM E CARACTERIZAÇÃO DO QUARTZO AZUL EM METARRIOLITOS DO GRUPO RIO DOS REMÉDIOS, PARAMIRIM (BA)

Dissertação apresentada ao Programa de Pós-Graduação em Geociências do Centro de Tecnologia e Geociências da Universidade Federal de Pernambuco, como requisito parcial para a obtenção do título de Mestre em Geociências.

Área de concentração: Geoquímica, Geofísica e Evolução Crustal.

Orientador: Prof. Dr. Lauro Cezar Montefalco de Lira Santos.

Coorientador: Prof. Dr. Pedro Luiz Guzzo.

Recife

2023

Catalogação na fonte:
Bibliotecária Sandra Maria Neri Santiago, CRB-4 / 1267

S586o Silva, Danielle Cruz da.
Origem e caracterização do quartzo azul em metarriolitos do grupo Rio dos Remédios, Paramirim (BA) / Danielle Cruz da Silva. – 2023.
70 f.: il., fig., e tab.

Orientador: Prof. Dr. Lauro Cezar Montefalco de Lira Santos.
Coorientador: Prof. Dr. Pedro Luiz Guzzo.
Dissertação (Mestrado) – Universidade Federal de Pernambuco. CTG. Programa de Pós-Graduação em Geociências. Recife, 2023.
Inclui referências.

1. Geociências. 2. Quartzo azul. 3. Inclusões. 4. Espelhamento da luz. 5. Rayleigh. 6. Metavulcânicas. I. Santos, Lauro Cezar Montefalco de Lira (Orientador). II. Guzzo, Pedro Luiz (Coorientador). III. Título.

UFPE

551 CDD (22. ed.) BCTG/2023-115

DANIELLE CRUZ DA SILVA

# ORIGEM E CARACTERIZAÇÃO DO QUARTZO AZUL EM METARRIOLITOS DO GRUPO RIO DOS REMÉDIOS, PARAMIRIM (BA)

Dissertação apresentada ao Programa de Pós-Graduação em Geociências da Universidade Federal de Pernambuco, Centro de Tecnologia e Geociências da Universidade Federal de Pernambuco, como requisito parcial para a obtenção do título de Mestre em Geociências.
Área de concentração: Geoquímica, Geofísica e Evolução Crustal.

Aprovada em: 14/02/2023.

**BANCA EXAMINADORA**

_____

Prof. Dr. Lauro Cezar Montefalco de Lira Santos (Orientador)
Universidade Federal de Pernambuco

_____

Profa. Dra. Adriane Machado (Examinador Externo)
Universidade Federal de Sergipe

_____

Profa. Dra. Cristiane Paula de Castro Gonçalves (Examinador Externo)
Universidade de Ouro Preto

_____

Prof. Dr. Haroldo Monteiro Lima (Examinador Interno)
Universidade Federal de Pernambuco

## AGRADECIMENTOS

Gostaria de agradecer, a todas as pessoas que participaram, direta ou indiretamente, desta etapa da minha vida e tornaram esse trabalho possível.

Primeiramente, aos meus pais Rosânia e Ailton, por todo apoio, amor e esforços investidos em mim e na minha educação. A minha família, principalmente meus avós por todos o carinho e apoio.

Agradeço a Matheus, por estar sempre ao meu lado, me apoiando e me aconselhando mesmo nos momentos difíceis e sempre quando preciso.

Agradeço ao meu orientador, Prof. Dr. Lauro Cézar Montefalco de Lira Santos, pela orientação, companheirismo e esforço, sempre fazendo com que o trabalho evoluísse.

Agradeço a coorientação do Prof. Dr. Pedro Luiz Guzzo por ter me recebido e pela orientação durante a execução do trabalho e pelo apoio logístico nas análises de espectroscopia e difração de raios-X.

Agradeço a Prof. Dra. Glaucia Queiroga e Prof. Dra. Mahyra Tedeschi por todo apoio nas análises de EPMA e Raman e pelas orientações ao longo do trabalho.

Agradeço a todos do Laboratório de Tecnologia Mineral (LTM), em especial à Marcelo, por todo o suporte e cuidado durante todo o tempo. E Paula e Filipe pela ajuda e amizade.

Ao Professor Patrick Cordier e à UFPE pela concessão de recursos e apoio logístico que possibilitaram a realização das análises de microscopia de transmissão na Universidade de Lille.

Agradeço à CAPES (Coordenação de Aperfeiçoamento de Pessoal de Nível Superior), fundação do Ministério da Educação (MEC), pelo apoio financeiro através da concessão da bolsa de mestrado.

Por fim, agradeço a todos os meus amigos Arthur, Ananda, Débora, Asayuki e João, pelo companheirismo, amizade e discussões, além de todo apoio ao longo de todos esses anos. Serei eternamente grata por todos os momentos que vocês me proporcionaram e por terem tornado essa caminhada mais leve.

“There is neither happiness nor misery in the world; there is only the comparison of one state with another, nothing more. He who has felt the deepest griefs best to able to experience supreme happiness” (DUMAS, A., 1846, p. 1080).

## RESUMO

As variedades do quartzo ocupam uma fração considerável da crosta continental, ocorrendo com abundância em vários tipos de rochas, como granitos, riolitos, gnaisses e rochas siliciclásticas. Apesar de ocorrer na maioria das vezes como cristais incolores, existem uma grande gama de variedades coloridas, o quartzo azul é uma delas. Cristais de quartzo com coloração azul é um raro componente de rochas ígneas e está presente principalmente em granitos, granodioritos, riolitos e charnoquitos, e seus equivalentes metamórficos. Apesar de pouco frequente, foram contabilizadas 245 ocorrências de quartzo azul no mundo, e o Brasil concentra um número considerável. O estado de Bahia concentra um grande número de ocorrências, as quais têm potencial de se tornar um indiciador para as condições de cristalização de rochas portadoras de quartzo azul. Este trabalho apresenta uma investigação integrada de diversas análises, sobre a caracterização e origem da ocorrência de quartzo azul em rochas metavulcânicas no sudoeste da Bahia. A mineralogia das rochas consiste essencialmente em fenocristais de quartzo e K-feldspato, imersos em uma matriz quartzo/felspastática e composta por biotita, muscovita, fluorita, alanita, clorita, zircão e minerais opacos. Análises de microssonda eletrônica revelaram a presença de dois tipos distintos de biotita (magmática e neoformada), de micas brancas ricas em ferro e de ortoclásio. Quando analisado os cristais de quartzo separadamente, as análises realizadas em diversas técnicas não foram capazes de apontar nenhuma característica distinta de aquelas presentes em cristais incolores. Apenas por meio da microscopia de transmissão foi possível constatar a presença de dois tipos de inclusões sólidas submicroscópicas ricas em Ti. Tal característica é recorrente em cristais de quartzo azul e origem da cor está associada ao processo de espelhamento da luz (espelhamento de Rayleigh) através das pequenas partículas. Acredita-se que a geração de tais inclusões se dá pelo processo de exsolução durante o crescimento e resfriamento do cristal. A mineralogia destas rochas está muito próxima a de magma peraluminosos e alcalinos, ricos em Ti, comuns em ambientes anorogênicos do tipo A. Tais configurações são terrenos férteis para a geração de rochas portadoras de quartzo azul.



Palavras-chave: quartzo azul; inclusões; espelhamento da luz; Rayleigh; metavulcânicas.

## ABSTRACT

Quartz varieties occupy a considerable fraction of the continental crust, occurring in abundance in various types of rocks, such as granites, rhyolites, gneisses, and siliciclastic rocks. Although it occurs most often as colorless crystals, there are a wide range of colored varieties, blue quartz being one of them. Blue colored quartz crystals are a rare component of igneous rocks and are mainly present in granites, granodiorites, rhyolites and charnoquites, and their metamorphic equivalents. Besides uncommon, 245 occurrences of blue quartz were recorded in the world, and Brazil concentrates a considerable number. The state of Bahia is an important representative due to the concentration of occurrences that have the potential to become an indicator for the conditions of crystallization of rocks bearing blue quartz. This work presents an integrated investigation of several analyses, on the characterization and origin of the occurrence of blue quartz in metavolcanic rocks in southwest Bahia. The mineralogy of the rocks essentially consists of quartz and K-feldspar phenocrysts, immersed in a quartz/felspastatic matrix, and composed of biotite, muscovite, fluorite, alanite, chlorite, zircon and opaque minerals. Electron microprobe analyzes revealed the presence of two distinct types of biotite (magmatic and neoformed), iron-rich white micas and orthoclase. When analyzing the quartz crystals separately, the analyzes carried out in different techniques were not able to point out any characteristic distinct from those present in colorless crystals. Only through transmission microscopy was it possible to verify the presence of two types of Ti-rich submicroscopic solid inclusions. This characteristic is recurrent in blue quartz crystals and the origin of the color is associated with the light mirroring process (Rayleigh mirroring) through small particles. It is believed that the generation of such inclusions is due to the exsolution process during crystal growth and cooling. The mineralogy of these rocks is very close to that of peraluminous and alkaline magma, rich in Ti, common in type A anorogenic environments. Such configurations are fertile ground for the generation of rocks bearing blue quartz.



Keywords: blue quartz; inclusions; light scattering; Rayleigh; metavolcanic.

## LISTA DE FIGURAS

## LISTA DE TABELAS

**SUMÁRIO**

# 1 INTRODUÇÃO

A ocorrência de variedades coloridas de cristais de quartzo é uma característica conhecida e altamente explorada, porém a variedade azul do quartzo é um componente atípico de rochas ígneas, se comparado com outras variedades de quartzo (cristal de rocha, quartzo leitoso, ametista, entre outros). Inúmeras variedades de rochas são hospedeiras de quartzo de cor azul, como granitos, granodioritos, riolitos, charnoquitos, assim como em anortositos e em produtos metamórficos (Zolensky *et al*., 1988).

Usualmente, a origem da coloração azul nos cristais de quartzo está associada à dois mecanismos principais: (i) à presença de minerais azulados no interior do quartzo, como dumortierita, aerinita e magnésio-ribeckita; e (ii) ao processo de espelhamento da luz (espelhamento de Rayleigh), devido à presença de inclusões submicroscópicas no interior dos cristais. As principais fases sólidas conhecidas são turmalina, a ilmenita, a biotita, a muscovita, a apatita e o zircão, incluindo também, o rutilo, que é o mais recorrente (Seifert *et al*., 2011).

A presente dissertação discorre a ocorrência de quartzo azul em rochas metavulcânicas basais do Grupo Rio dos Remédios. Essa ocorrência está localizada na microrregião do munício baiano de Paramirim. Neste sentindo, foram utilizadas diversas técnicas espectroscópicas, estudos químicos, análises qualitativas, microestruturais e gemológicas, a fim de caracterizar as rochas hospedeiras e definir os parâmetros de geração dos cristais azulados de quartzo.

## 1.1 JUSTIFICATIVA

O Grupo Rio dos Remédios, localizado na porção centro-leste do Estado da Bahia, compreende rochas metavulcânicas ácidas a intermediárias, com intercalações de rochas piroclásticas e quartzíticas (Pedroza *et al.,* 1999), que foram formadas a partir de rifte intracontinental mesoproterozoico (Oga, 1997). As rochas metavulcânicas apresentam como características, a textura porfirítica e a presença de fenocristais de feldspato e quartzo de tonalidades azuladas.

Apesar da tonalidade azulada do quartzo ser uma característica relevante mineralogicamente e ser um fato conhecido, os estudos quanto a origem e desenvolvimento dos cristais desta cor são ausentes. Desta forma, faz-se necessário maiores estudos quanto a

ocorrência de quartzo azul e suas rochas hospedeiras, com ênfase na ocorrência do quartzo azul e a correlação com o tipo de ambiente geotectônico e mineralizações associadas.

## 1.2 OBJETIVOS

O objetivo geral da dissertação é compreender os mecanismos geradores da coloração azul nos cristais de quartzo dos metarriolitos do Grupo Rio dos Remédios e traçar correlações entre a cor e as condições geológicas de formação desses cristais. Os objetivos específicos incluem: (i) ampliar a amostragem e estabelecer as principais relações de campo entre as rochas portadores dos cristais de quartzo e encaixantes; (ii) realizar descrições petrográficas meso- e microscópica de amostras representativas, respeitando as variações texturais, estruturais e propriedades físicas gerais dos cristais de quartzo; (iii) identificar a presença de possíveis inclusões nos cristais de quartzo azul, além de determinar a composição química dos cristais e suas inclusões.

## 1.3 LOCALIZAÇÃO E VIAS DE ACESSO

A área de estudo se localiza no sudoeste do Estado da Bahia, a cerca de 7 km do centro do distrito de Canabravinha, município de Paramirim, distante aproximadamente 1.400 km da capital do Estado de Pernambuco, Recife. Partindo de Recife o acesso à área (Fig. 1) se dá a partir da BR-232, até o município de Caruaru e seguindo pela BR-423 até Paulo Afonso, cruzando Garanhuns. A partir deste ponto o trajeto continua pela BR-110, e pela BR-116 cruzando a cidade de Feira de Santana até ao entroncamento que dá acesso a BR-30, seguindo em direção a cidade de Brumado. A partir desta cidade, a viagem continua pela BA-148 até o Município de Livramento de Nossa Senhora. A área de estudo está a cerca de 54 km de distância do povoado. Os afloramentos visitados se encontram no interior do povoado e podem ser acessados por estradas secundárias e não pavimentadas.

Figura 1 - Principais vias de acesso partindo de Recife (PE) para a cidade de Paramirim (BA).

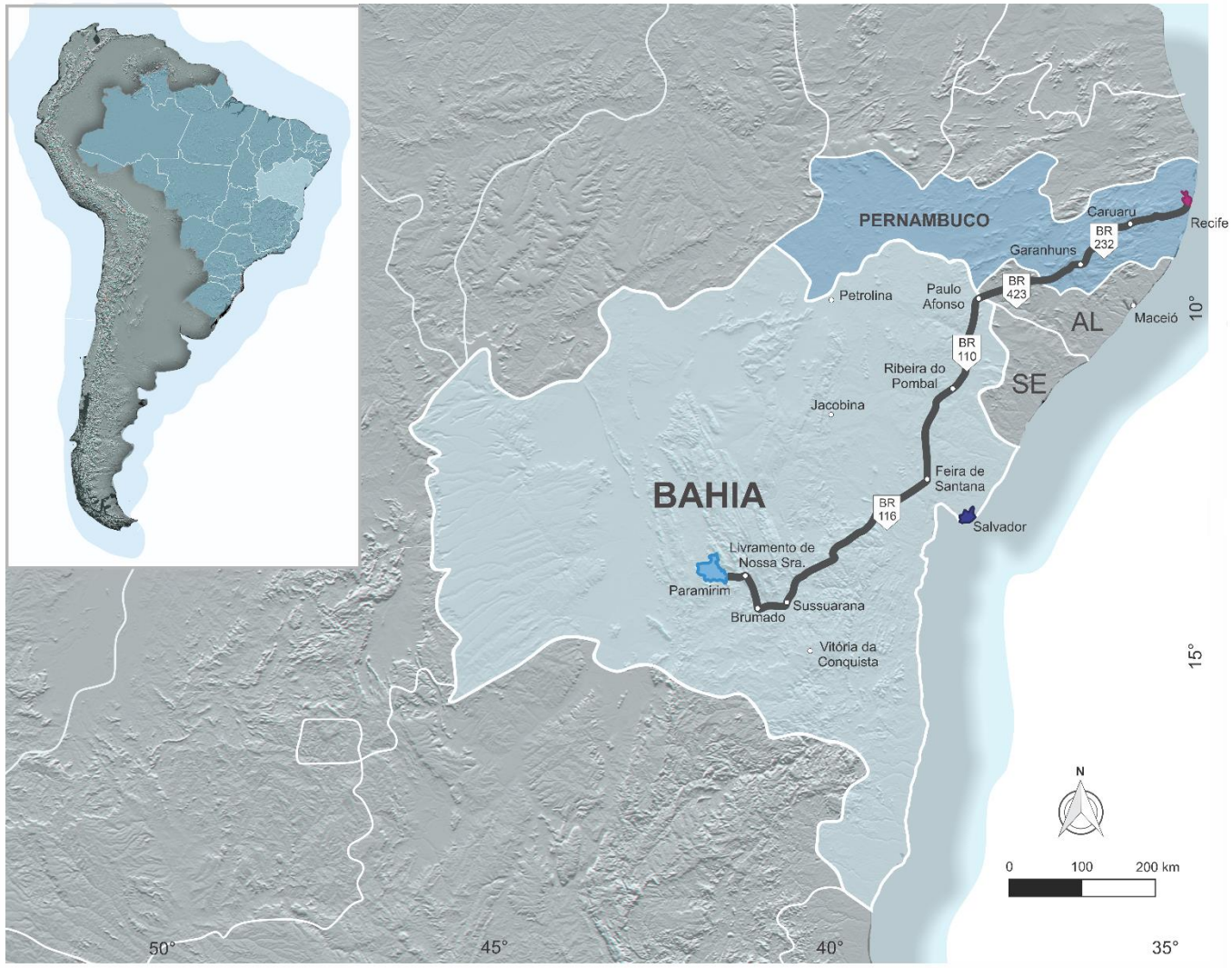


Fonte: O Autor (2023).

# 2 MULTI-METHOD CHARACTERIZATION OF RARE BLUE QUARTZ-BEARING METAVOLCANIC ROCKS OF THE RIO DOS REMÉDIOS GROUP, PARAMIRIM AULACOGEN, NE BRAZIL

Danielle Cruz da Silva[1*], Lauro Montefalco[1], Gláucia Queiroga[2], Glenda Lira Santos[1], Mahyra Tedeschi[3]

[1] Departamento de Geologia, Universidade Federal de Pernambuco–Recife (PE), Brasil. E-mails:danielle.cruz@ufpe.br, dani.cs8@live.com, lauro.lsantos@ufpe.br, glenda.lira@ufpe.br

[2] Departamento de Geologia, Escola de Minas, Universidade Federal de Ouro Preto–Ouro Preto (MG), Brasil.E-mail:glauciaqueiroga@ufop.edu.br

[3] Programa de Pós-Graduação em Geologia, Universidade Federal de Minerais, Centro de Pesquisas Manoel Teixeira da Costa, Instituto de Geociências, Universidade Federal de Minas Gerais–Belo Horizonte (MG), Brasil. E-mail:mahyratedeschi@gmail.com

*Corresponding author.

## ABSTRACT

The Rio dos Remédios Group comprises a supracrustal sequence that occupies the base of the Espinhaço Supergroup, São Francisco Craton, Brazil. Its basal formation, Novo Horizonte, crops out in the Paramirim region mainly as metavolcanic rocks that represent one of the fewer occurrences of blue quartz phenocrysts in South America. Their mineralogy consists of quartz and K-feldspar phenocrysts, whereas biotite, muscovite, fluorite, allanite, chlorite, sericite, zircon, and opaque phases occur immersed in a quartz-feldspar-rich groundmass. This composition is also supported by x-ray diffraction and chemical data. Electron probe microanalysis in some samples revealed the presence of two distinct groups of biotite (magmatic and neoformed), in addition to the presence of iron-rich white mica and almost pure orthoclase feldspar. Our data suggest that the studied metavolcanic rocks have maintained their magmatic characteristics, which were progressively overprinted by hydrothermal fluids and ductile-to-brittle deformation. The magmatic mineralogy is akin to strongly peraluminous and alkaline magmas, common inanorogenic settings–a fertile site for the origin of blue quartz-bearing rocks worldwide.

**KEYWORDS**: blue quartz-bearing rocks petrology; Paramirim Aulacogen; São Francisco Craton

## 1 INTRODUCTION

Blue quartz is a rare component of igneous rocks whose origin was formerly discussed in the classical work by Iddings (1904), who suggested that its color results from light scattering due to high concentrations of submicron-sized solid inclusions. So far, there is no consensus regarding the nature of the inclusions in blue quartz (for discussion, see Seifert *et al*.2011). It has been proposed, however, that the blue color usually reflects the presence of tiny crystals of rutile, ilmenite, magnetite, graphite, biotite, zircon, apatite, tourmaline, or magnesio-riebeckite (Pantia *et al*.2019).

Although uncommon in the continental crust, blue quartz crystals are reported in several common lithotypes, including granites, granodiorites, rhyolites, charnockites, and the metamorphosed products of these rocks,covering approximately 245 occurrences around the world (Pantia *et al*., 2019).Alkaline igneous rocks and their metamorphic correspondents are considered the most fertile sources for the occurrence of this mineral variety (Seifert *et al*., 2011). This association might be explained by unique aspects of the source, including distinctive geochemical character (e.g., metaluminous and peralkaline) and the high temperature of the progenitor magma (Gao *et al*.2020), which are appropriate conditions favoring the greater inclusion in the blue quartz.

The Paramirim region in NE Brazil is characterized by metavolcanosedimentary sequences, including the Rio dos Remédios Group, which hosts mainly porphyritic metavolcanic rocks composed of centimetric (~2 cm) blue quartz phenocrysts, as previously described by Cavalcanti *et al*. (1980). It is suggested that such rocks represent precursor A-type peraluminous magmas, which occupy the base of a thick succession of acid lavas and siliciclastic metasedimentary rocks (e.g., Guimarães *et al*., 2008; Heilbron *et al*., 2017). Among the most famous blue quartz-bearing rocks in South America, such metavolcanic rocks remain poorly investigated, as detailed petrographic/mineralogical studies, as well as the investigation of the possible origin of the blue quartz coloration, have not yet been conducted. As a result, there is a major knowledge gap in the basic characterization of such unique rocks in the continental crust.

This study aimed to present the first petrological-chemical study of the metavolcanic rocks that host blue quartz phenocrysts of the Rio dos Remédios Group in the Paramirim

region, based on detailed petrographic descriptions, X-ray diffraction (XRD), and mineral chemistry. We focus on the major compositional aspects of these rocks, also presenting inferences about their magmatic sources and comparing our occurrences to worldwide examples of (meta)volcanic rocks, which will help further studies about the origin of blue quartz.

## 2 GEOLOGICAL SETTING

The study area is in the morphotectonic domain of the Paramirim Aulacogen, in the Northern portion of the São Francisco Craton (Fig. 2). This cratonic block represents a large lithospheric segment composed of Archean terranes that were assembled during subduction-collision events between 2.1 and 2 Ga (Almeida, 1977; Barbosa and Sabaté2003). In terms of reconstructions of Western Gondwana, this craton is limited by Neoproterozoic orogenic domains, including the Araçuaí, Brasília, Rio Preto, Riacho do Pontal,and Sergipano fold belts(Cruz and Alkmim, 2007, Rosa, 1999, Heilbron *et al*, .2017; Caxito *et al*., 2020). The Paramirim Aulacogen represents an NNW-oriented intra continental rift system developed from a succession of syneclysis aged between 1.70 and 0.65 Ga (Alkmim *et al*., 2007; Danderfer *et a*l., 2014; Santana, 2016). In a simplified view, it comprises two major lithostratigraphic units:

- The Espinhaço Supergroup (Schobbenhaus, 1996);
- The São Francisco Supergroup (Cruz *et al*, .2007).

Both successions were strongly deformed via tectonic inversions that took place during the Neoproterozoic (Guimarães *et al*., 2005, 2012; Guadagnin and Chemale Jr., 2015; Cruz and Alkmim, 2017) and are interpreted as the result of the Brasiliano-PanAfrican Orogeny (0.8–0.5 Ga; Brito Neves *et al*., 2014), resulting in the development of the intracontinental Paramirim corridor (Alkmim *et al*., 1993; Carlin *et al*., 2018).

The Espinhaço Supergroup is interpreted as a metavolcanosedimentary sequence of predominantly terrigenous and metasedimentary rocks, with acid to intermediate volcanic contributions, mainly at its basal portion (Cruz *et al*., 2007; Medeiros, 2013). It comprises the chapada Diamantina, Paraguaçu, Rio dos Remédios and Serra da Gameleira sequences (Fig. 3).

The Rio dos Remédios Group encompasses metavolcanic, pyroclastic and sedimentary rocks, mainly represented by a succession of acid lavas and lacustrine to alluvial sediments, overlaying the sedimentary rocks of the Serra da Gameleira sequence. According to

Schobbenhaus and Kaul (1971), this sequence represented the initial stage of rifting, marked by volcanic rocks interleaved with clastic members that encompass the siliciclastic sequence (Guimarães *et al*., 2005; Teixeira, 2005; Loureiro *et al.*, 2008; Cruz and Alkmim, 2017).

The oldest volcanism of the Rio dos Remédios Group is represented by alkaline A2-type rocks of the Novo Horizonte Formation (Teixeira, 2005), crystallized between ca. 1752 and 1748 (U/Pb in zircon) (Babinski *et al*., 1994; Schobbenhaus *et al*., 1994), whereas the upper units, Lagoa de Dentro/Ouricuri do Ouro Formation, host the pure sedimentary components of the group.

In the study area, metavolcanic members of Novo Horizonte Formation include porphyritic metadacites, metarhyolites, and meta-andesites, usually modified by pervasive deformation and fluid influence of both magmatic and metamorphic origins (Danderfer and Dardenne, 2002; Barbosa, 2012, Santos *et al*., 2019). The metavolcanic rocks crop out as slightly to moderately deformed blocks and boulders of dominant grayish colorations with mesoscopic porphyritic texture, mostly marked by feldspar and blue quartz phenocrysts.

**Figura 1 -** SRTM map of the São Francisco Craton showing the bordering Neoproterozoic Brasiliano belts, the morphotectonic domain of the Paramirim aulacogen, the proterozoic cover sequence (younger than 1.8 Ga) of the Espinhaço Supergroup and the sampling location.

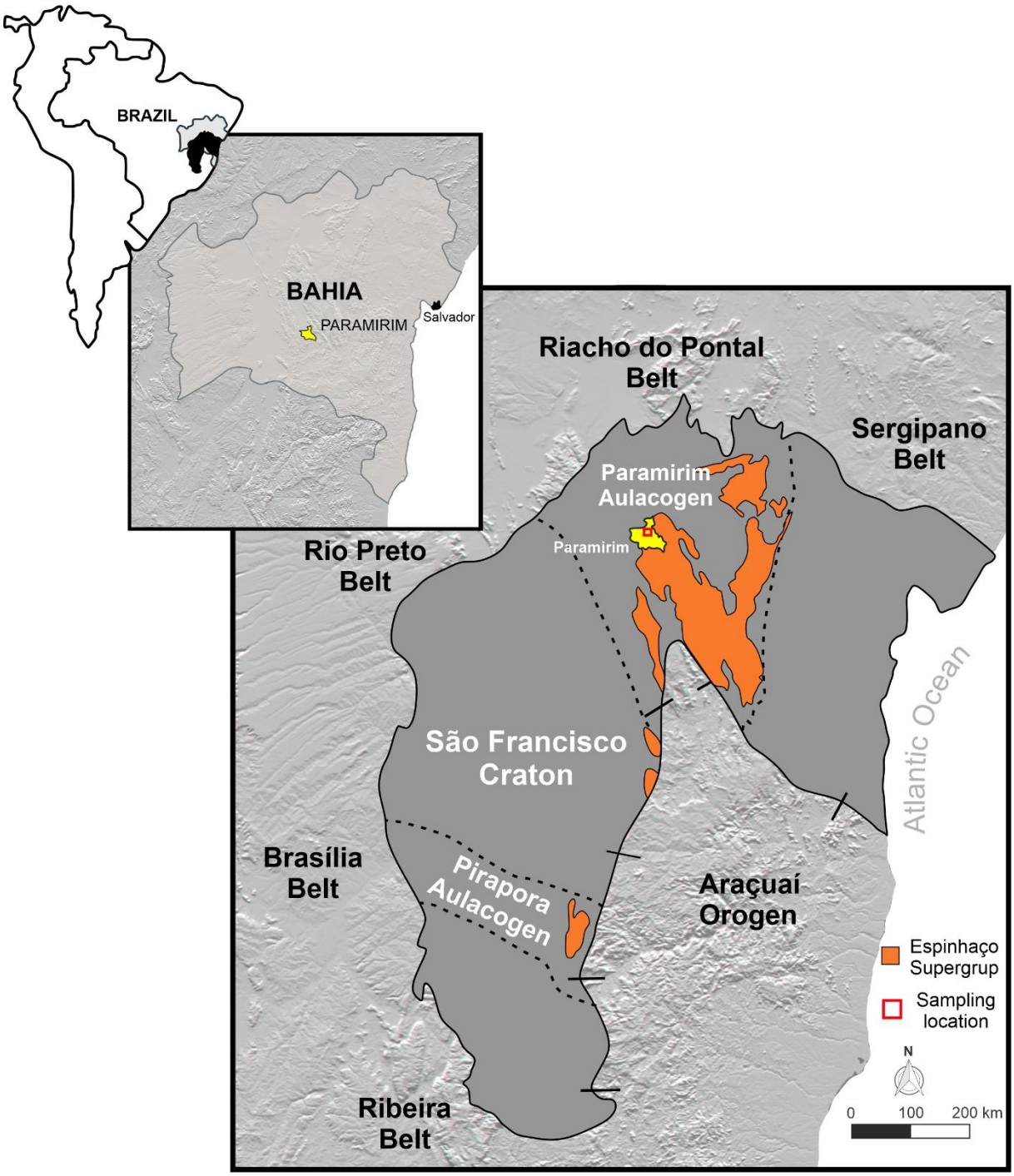


**Source:** Modified from Alkmin *et al*. (2007).

**Figura 2 -** Geological map of the Espinhaço Supergroup in the Southeast of Bahia region highlighting the Rio dos Remédios Group and the sampling location; modified from Arcanjo *et al*. (1999).

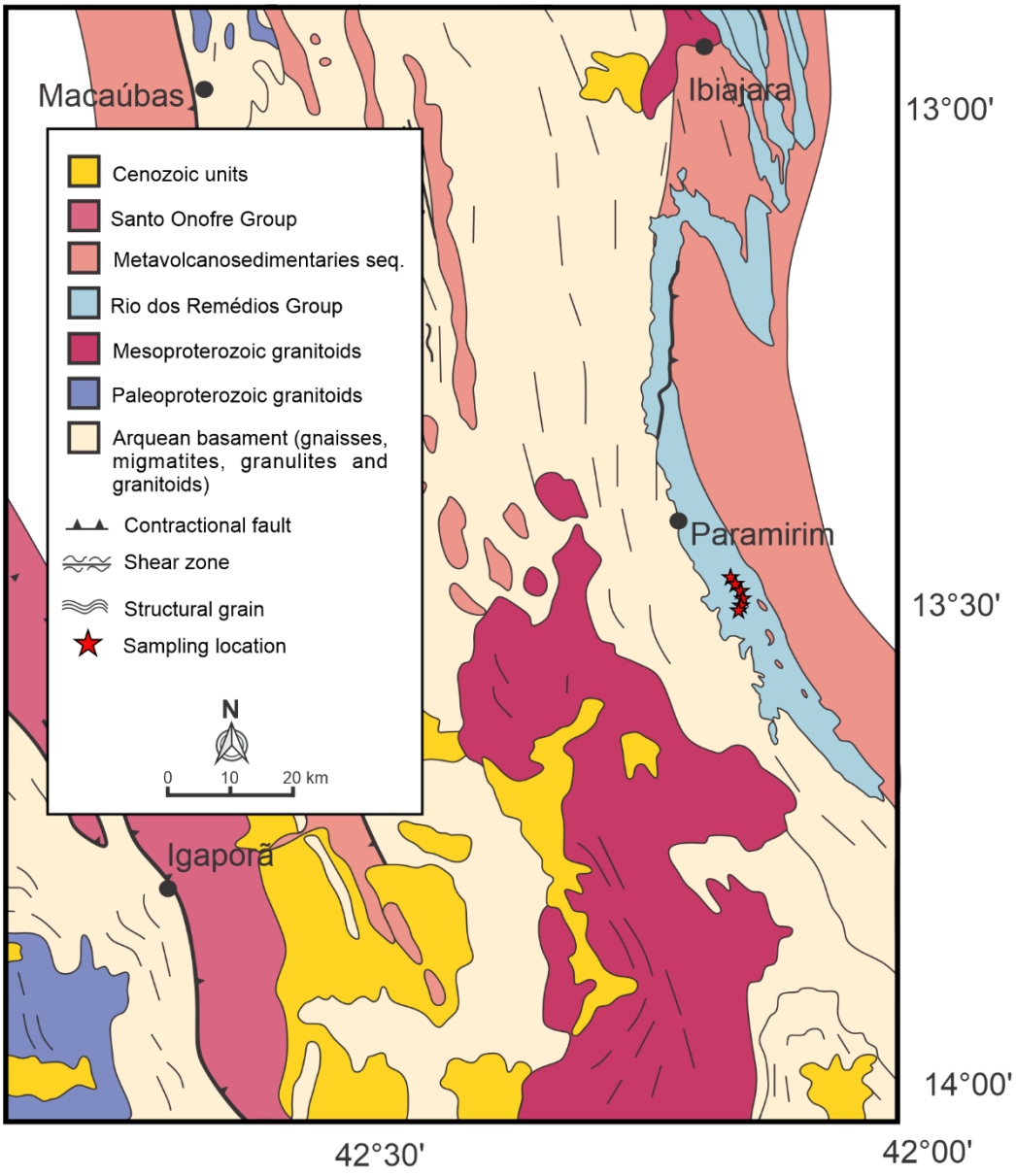


**Source:** modified from Arcanjo *et al*. (1999).

## 3 METHODOLOGY

### *Sample selection*

Ten thin sections were selected for petrographic analysis using an Olympus BX51 microscope with an Olympus DP26 camera, at the Gemology Lab of the Universidade Federal de Pernambuco (UFPE), Brazil. Four representative polished thin sections (P4, P5, P6, and P7) were chosen for detailed analysis with XRD, scanning electron microscopy (SEM), and electron microprobe.

***X-ray diffraction***

The XRD measurements were taken at the Laboratório de Tecnologia Mineral,UFPE, Brazil. The analyses of four samples were performed on a Bruker D2 PHASERusing Cu-Kα radiation equipped with a Bruker-AXS-Lynxeye detector. The voltage, radiation, and current of the generator were set at 30 kV, 1.54060 Å,and 10 mA (p=300W),respectively. The diffraction pattern was recorded for 2θ from 4°to 80°with a step scan of 0.02019°in a constant rotation of 10 rpm, counting for 1.5 s at every step. The results were indexed using the app DIFFRAC.EVA with the database COD (REV212673 2018.12.20).

***Scanning electron microscopy analysis***

The SEM analysis was carried out at the Laboratório de Micropaleontologia Aplicada (LMA), UFPE, Brazil. The four thin sections were selected for image acquisition and qualitative analysis, using a Phenom XL with a back scattered electron detector. The tension, radiation, and current of the generator were set at 15 kV.

***Electron probe micro-analyses***

The four selected polished thin sections were analyzed using a JEOL JXA-8230 superprobe in the Microscopy and Microanalysis Laboratory at the Universidade Federal de Ouro Preto (UFOP), Brazil. Analyses were conducted at an acceleration voltage of 15 kV, a current of 20nA, and spot sizes of 5–10 μm. The analyzed elements and instrumentation standards were as follows: Si (quartz), Na (anorthoclase), K (microcline), Mn (MnO2), Mg (olivine), Ca (fluorapatite), P (fluorapatite), Al (corundum), Fe (metallic Fe), F (CaF2), Cl (scapolite), Ba (BaSO4), Cr (chromite), Sr (strontianite), Ti (rutile), and Zn (gahnite). Counting times on peak and background were 10 and 5 s, respectively, for all elements. ZAF (atomic number, absorption, fluorescence) was the applied common matrix correction.

## 4 RESULTS

***Field aspects***

The studied metavolcanic rocks crop out as highly deformed large blocks and boulders (~2 m long) with common spheroidal exfoliation along foliation planes that follow the NNE-SSW regional trend typical of the Novo Horizonte Sequence (Figs. 4Aand 4B). They exhibit a grayish to dark gray color and shades of reddish and greenish yellow when weathered. The

rocks are holocrystalline and often porphyritic with phenocrysts of reddish feldspar and opalescent blue quartz phenocrysts (Fig. 4C).

Unlike deformed granitoids, quartz phenocrysts in volcanic rocks maintain their primary volcanic characteristics in intense ductile deformation (Etheridge and Vernon, 1981; Williams and Burr1990), whereas K-feldspar phenocrysts may also be preserved in varying degrees of deformation. Thus, a classical phenocryst classification was used in this work since they represent relic crystals of the deformed volcanic rocks (Vernon, 1990).

Quartz phenocrysts exhibit subhedral to anhedral shapes, also occurring as hexagonal bipyramids, ranging from 0.03 to 0.50 cm in diameter. They normally occur surrounded or embayed by the rock matrix. Crystals are mainly milky blue, often eventually exhibiting dark blue rims. The feldspar phenocrysts occur as 4-mm-to 15-cm-long subhedral to euhedral crystals, exhibiting tabular habits. A slightly developed flow orientation is marked by the alignment of elongated eye-shaped crystals. Contrastingly to the quartz crystals, K-feldspar forms clusters of parallel crystals, mostly associated with widespread mineral aggregates (Fig. 4D).

The dominant rock groundmass is grayish to locally light brown, being composed of fine-grained quartz + feldspar aggregates, as well as clusters of biotite, chlorite, and sericite lamellae. All studied rocks are widely fractured, including fine-grained mineral clusters that filled the fracture planes, but the mylonitization effect has not been identified.

**Figura 3 -** Field and mesoscopic aspects of the Rio dos Remédios metarhyolites. Rocks from the Rio dos Remédios Group are exposed as (A) rhyolitic layers and (B) as massive blocks. (C) Porphyritic microstructure highlighting blue quartz and K-feldspar phenocrysts in a deformed metavolcanic sample. (D) Features of the felsitic groundmass and characteristics of the K-feldspar phenocrysts as clusters of parallel crystals (yellow arrow).

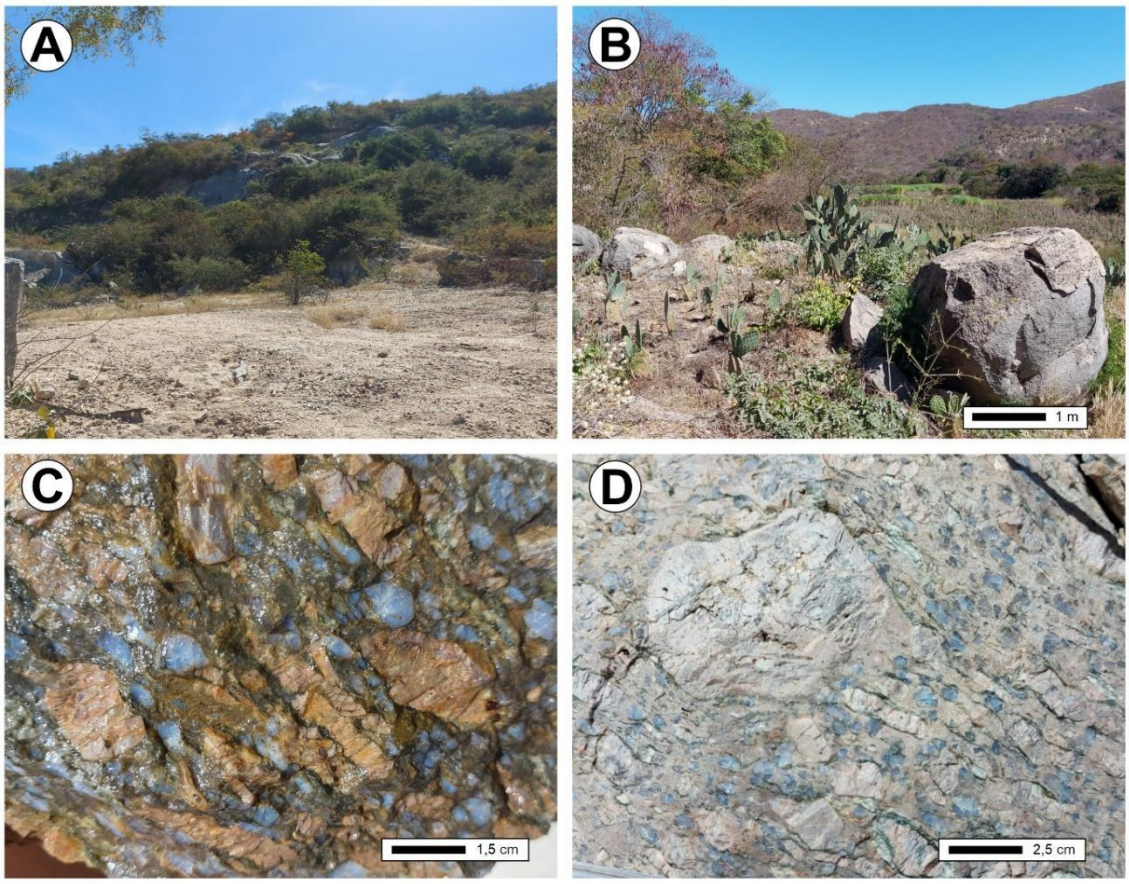


**Source:** Author (2022).

***Mineralogy, petrography and x-ray measurements***

In thin sections, the studied metavolcanic rocks show a dominant grayish color and microstructure that resembles the original porphyritic to phaneritic igneous texture. They exhibit well-formed quartz and feldspar phenocrysts, which are surrounded by a thin leucocratic groundmass.

Quartz and K-feldspar are the dominant phases, forming most of the rock phenocrysts with subhedral to anhedral crystalline habits and accounting for30% of the rock mode. The very fine-grained matrix is composed of quartz, K-feldspar and smaller amounts of biotite, zircon, white mica, fluorite and carbonate. In addition, the main opaque minerals are magnetite, ilmenite and unidentified iron oxide thin films. The deformation record is well

presented on quartz-feldspar-rich groundmass, which is highly affected by deep-seated tectonic processes. In addition to δ and σ porphyroclasts, the groundmass exhibits several deformation markers, including submillimeter-sized quartz-feldspar clots, with rounded shapes and diffuse contacts within thin and strongly recrystallized areas.

Quartz occurs as part of the groundmass and as anhedral porphyroclasts. Their diameter varies from 1 to 5 mm, but larger crystals might be locally observed. Quartz porphyroclasts exhibit rounded to subrounded shapes, also including engulfment textures, which are typical of (meta)volcanic rocks with high silica content (e.g., Silva *et al*., 2016). Magmatic corrosion is widespread, whereas undulose extinction and subgrain rotation are the main markers of the imposed regional deformation (Figs. 5A and 5B). Associated with the edges of the porphyroclasts are crystals formed by subgrain rotation recrystallization, with the same characteristics. Several fractures and microcracks are present and might be filled by epidote, chlorite, carbonate, muscovite, sericite, and micro-crystallized quartz veins.

Similar to the quartz, K-feldspar occurs as subhedral to anhedral megacrystals, presenting up to 0.8mm in length, and as scattered small crystals in the rock matrix. The crystals are commonly aligned with the primary magmatic flow structures in volcanic rocks and might exhibit well-developed Carlsbad twinning, as well as granophyric and perthite textures (Fig.5C).

Plagioclase is almost absent in all studied samples, occurring as anhedral to well-formed prismatic crystals. In addition, albite law twinning (Fig.5C) might be present but is not common. Both feldspar specimens are strongly affected by later alteration (i.e., sericitization and saussuritization) that might reach up to 60% of the crystals. In all samples, this process may be associated with the formation of secondary phases, including carbonate, sericite, and indistinct iron oxides.

Biotite is subhedral to anhedral, light brown to dark brown, and partially chloritized. The crystals form bent-flake lamellae aggregate on the edges of the major crystals, also occurring as inclusions in K-feldspar. It also occurs in contact with muscovite-bearing veins, also containing fluorite, sericite, and variable Fe-Ti oxides (Figs. 6A and 6B). Colorless fluorite is disseminated in the matrix as subhedral crystals, typically 0.1mm long, and occurs on the edge of micro-crystallized quartz veins within the K-feldspar crystals.

Muscovite occurs as very thin lamellae forming oriented veins along the matrix or surrounding the quartz and feldspar grains, also strongly oriented by the rock metamorphic foliation (Fig. 6C). Zircon, when present, exhibits prismatic and subhedral habits, ranging in

size from 0.01 to 0.04 mm, mostly as inclusions in the quartz crystals as well as forming halos on biotite lamellae.

Allanite is present as euhedral to subhedral dark brown crystals. It usually occurs dispersed in the matrix but may form isolated crystals on the edge of phenocrysts (Fig. 6D). Titanite and rutile subhedral crystals are not common but might occur in magnetite-and ilmenite-bearing samples. They usually attain 0.8 mm in length, showing subhedral to euhedral habits, also occurring as tiny inclusions on the phenocrysts.

In most samples, zircon, fluorite, carbonate, magnetite, and ilmenite range in size from 0.02 to 1 mm, occurring as disseminated tiny crystals within the rock groundmass as well as inclusions in quartz and K-feldspar in a lesser extent (Fig. 7). Even though there are several inclusions in quartz, their size is not compatible with the size described for Rayleigh scattering in minerals, ranging between 55 and 27 nm (Dörfler, 2002). Further studies, using transmission electron microscopy, are necessary to be able to identify and analyze the causes of the blue coloration.

**Figura 4 -** Photomicrographs with cross polarized from representative samples of the Rio dos Remédios Group metarhyolites. (A) Quartz (Qz) phenocrysts showing rounded to subrounded shapes, undulose extinction and fractures (B) also displaying engulfment textures. (C) K-feldspar (Kfs) phenocryst exhibiting granophyric texture and (D) plagioclase (Pl) crystal with well-developed albite twinning.

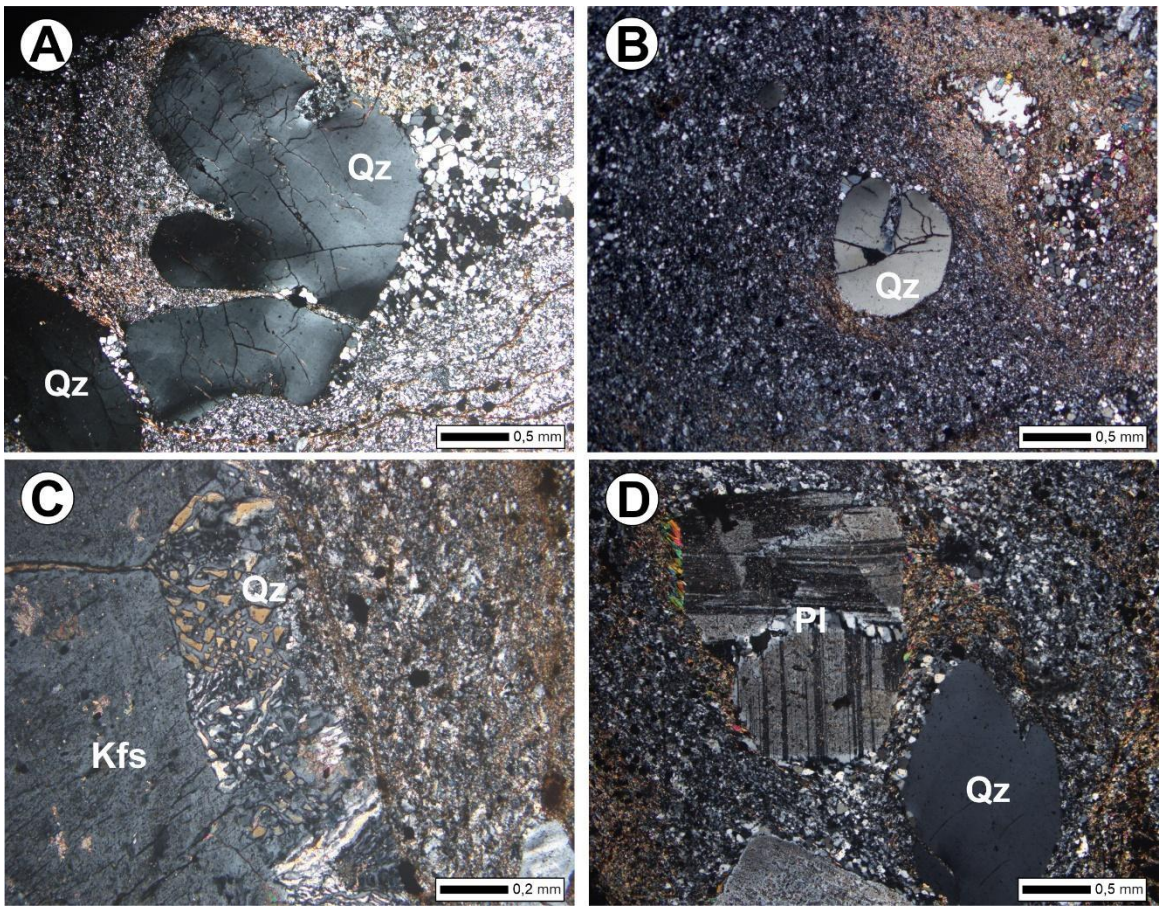


**Source:** Author (2022).

**Figura 5 -** Representative plane polarized light microphotographs (A, B, C, E) and SEM images (D, F). (A) and (B) Characteristics of the biotite (Bt) crystals, strongly chloritized, forming aggregates on the edge of the phenocrysts, usually associated to sericite (Ser), K-feldspar (Kfs), fluorite (Fl). (C) Oriented veins of muscovite (Ms) as part of the ground mass and (D) Overview of the allanite crystals associated with the Fe-Ti opaque components.

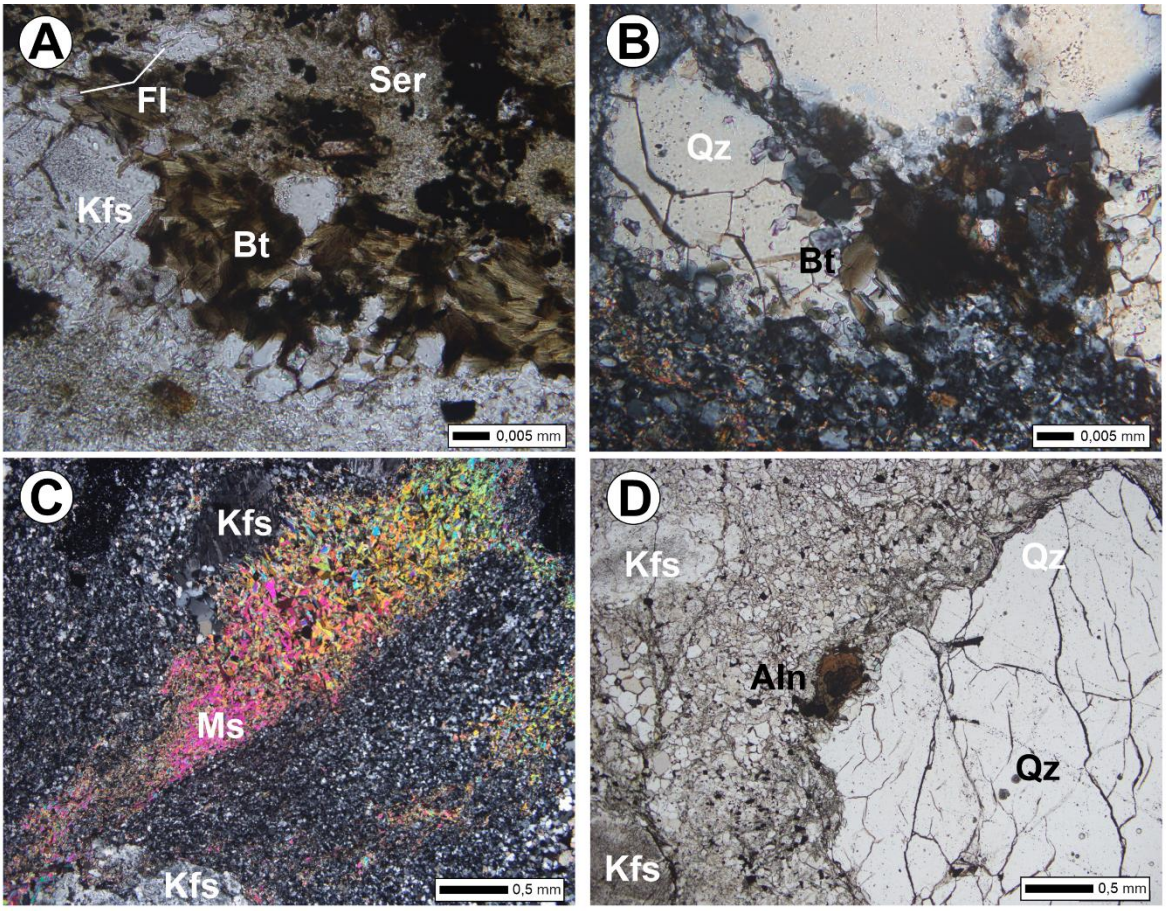


**Source:** Author (2022).

**Figura 6 -** Scanning electron microscopy images of inclusions present in quartz. (A) Microinclusions of zircon (Zr), (B) Illmenite (Ill) and (C) fluorite (Fl), carbonate (Cb) and presence of overgrown K-feldspar (Kfs).

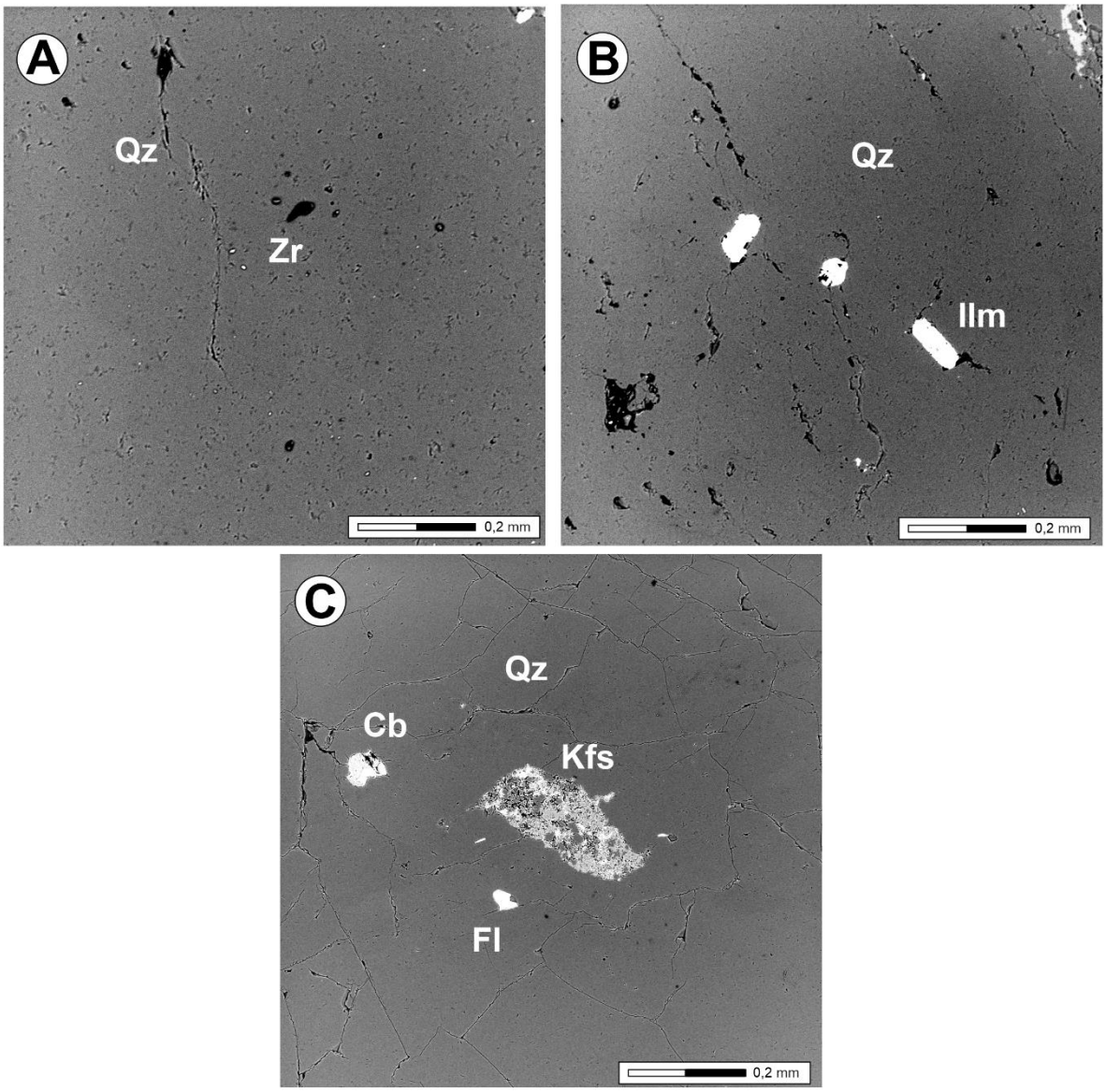


**Source:** Author (2022).

Whole-rock XRD analyses were performed to enhance the mineralogical control of the studied samples of rock blue quartz-bearing metarhyolites. The obtained results are in accordance with the mineralogy described in the petrographic analysis (Fig. 8). The presented diffractograms were indexed according to Wright and Stewart (1968), in which quartz, biotite, albite, microcline and oligoclase mineral phases were the main rock components. Furthermore, there is a predominance of microcline peaks (M)and, to a lesser extent, albite

peaks (A), which possibly represent the albite intergrown in the K-feldspar, not identifiable in the petrographic investigation.

**Figura 7 -** Representative diffractogram of the Rio dos Remédios metarhyolite. The main mineral phases are quartz, microcline, oligloclase, albite and biotite.

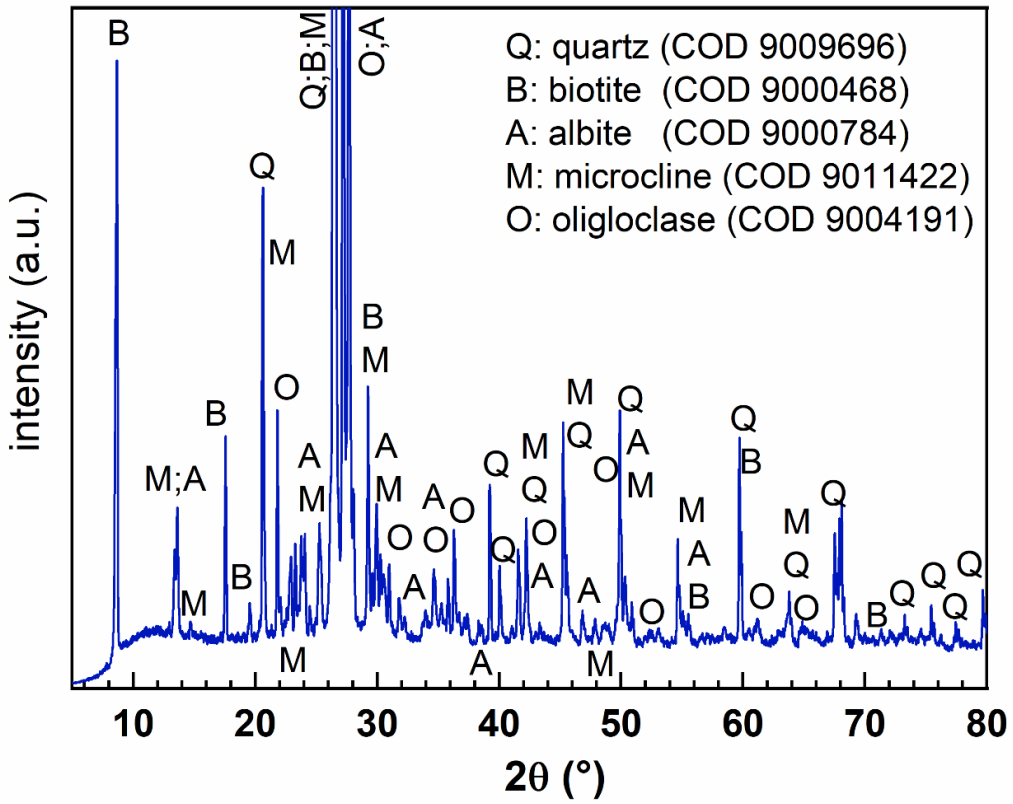


**Source:** Author (2022).

***Mineral chemistry***

Feldspar phenocrysts are mostly pure orthoclase (Or96.5–98.1Ab1.6–3.4 An0.1), with of formula unit (Na0.02–0.04K0.98–1.02) Al0.97–1.02$Si_3O_8$, thought one sample has a sanidine chemical affinity (Or69.1Ab30.9) (Fig. 9A). The BaO content varies from 0.05 to 0.25%, whereas $K_2O$ varies from 11.5 to 17% and $Na_2O$ between 0.18 and 3.4% (Tabela 1).

The white mica, previously interpreted as primary muscovite in the petrography, has relatively high contents of FeO and low contents of MgO with an average formula unit of K0.85–0.96Al1.23–1.61(Si3.20–3.72Al0.27–0.79O20) (OH, F) (Table 2). According to the Guidotti (1987) diagram, most samples plot within the muscovite group field, exhibiting chemical similarities with ferrimuscovite and ferriphengite compositions, whereas one plot fits with pure phengite (Fig. 9B).

The analyzed biotite flakes (Tab. 3) can be classified into two groups. In the ternary diagram of Nachit *et al*. (2005), the data reflect differences on the basis of TiO2, FeO, MnO, and MgO contents. Group I can be classified as primary biotite, whereas group II crystals fit within neoformed biotite (Fig. 10A).

Group I micas are akin to phlogopite-rich members in the solid solution annite-phlogopite, with X Mg varying between 0.03 and 0.04 and X Fe varying from 0.79 to 0.81. The average formula unit is (Na0.00–0.01K0.95–1.00Ca0.00–0.001)(Al0.24–0.29Mg0.10–0.11Fe2.19–2.29)(Al0.24–0.29Si2.74–2.80)O10(OH,F)2. Considering the relationship of IV Al versus Fe/(Fe+Mg), group I biotite is mainly characterized by phlogopite and eastonite compositions (Fig. 10B), while members of group II have considerably higher FeO content, coupled with low concentrations of $TiO_2$, which is akin to the chamosite endmember, also characterized by Fe/(Fe+Mg) ratios of around 0.99.

The chlorite classification diagram shows the compositional variation between primary magmatic and chloritized biotite crystals, which reflects differences in iron, magnesium, and aluminum contents. For instance, changes between Mg and Fe indicate a replacement process that resulted in Fe-rich chlorite pseudomorphs (Fig. 10C), whereas the observed changes on Na and K contents represent the losses during chloritization (Wu *et al*., 2019).

**Figura 8 -** (A) An-Ab-Or ternary diagram for feldspar classification (Deer *et al*. 1992); (B) Muscovite chemical classification diagram (Guidotti, 1987). Mu: muscovite, Ph: phengite, FPh: ferriphengite, Fmu: ferrimuscovite, F*Um: second type of ferrimuscovite.

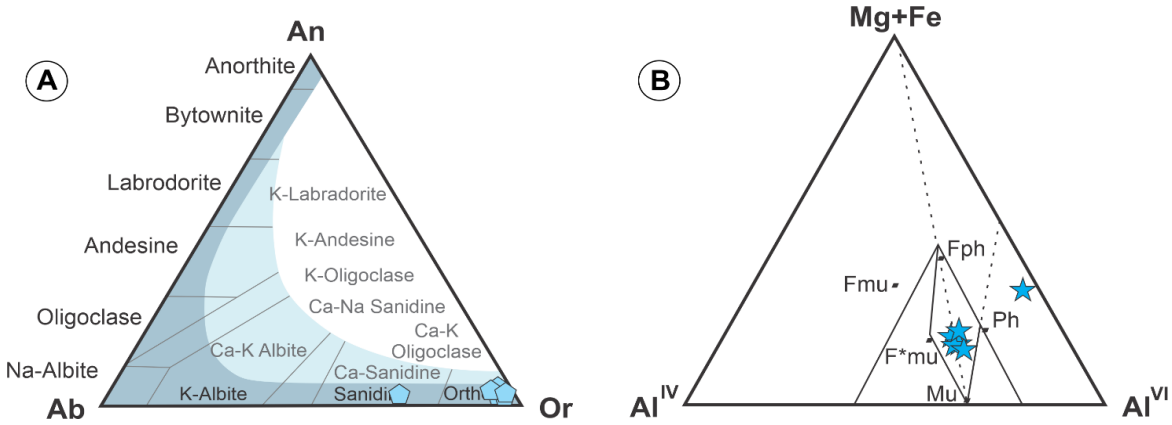


**Source:** Author (2022).

**Figura 9 -** (A) Fe# vs. AlIV for biotite classification (Deer, 1992). (B) TiO2-FeOt-MgO ternary diagram for biotite classification (Nachit et al., 2005); (C) (Al+□) -Mg-F compositional classification diagram of chlorite (Zane and Weiss, 1998). □ represents structure vacancies. Black dots represent endmembers.

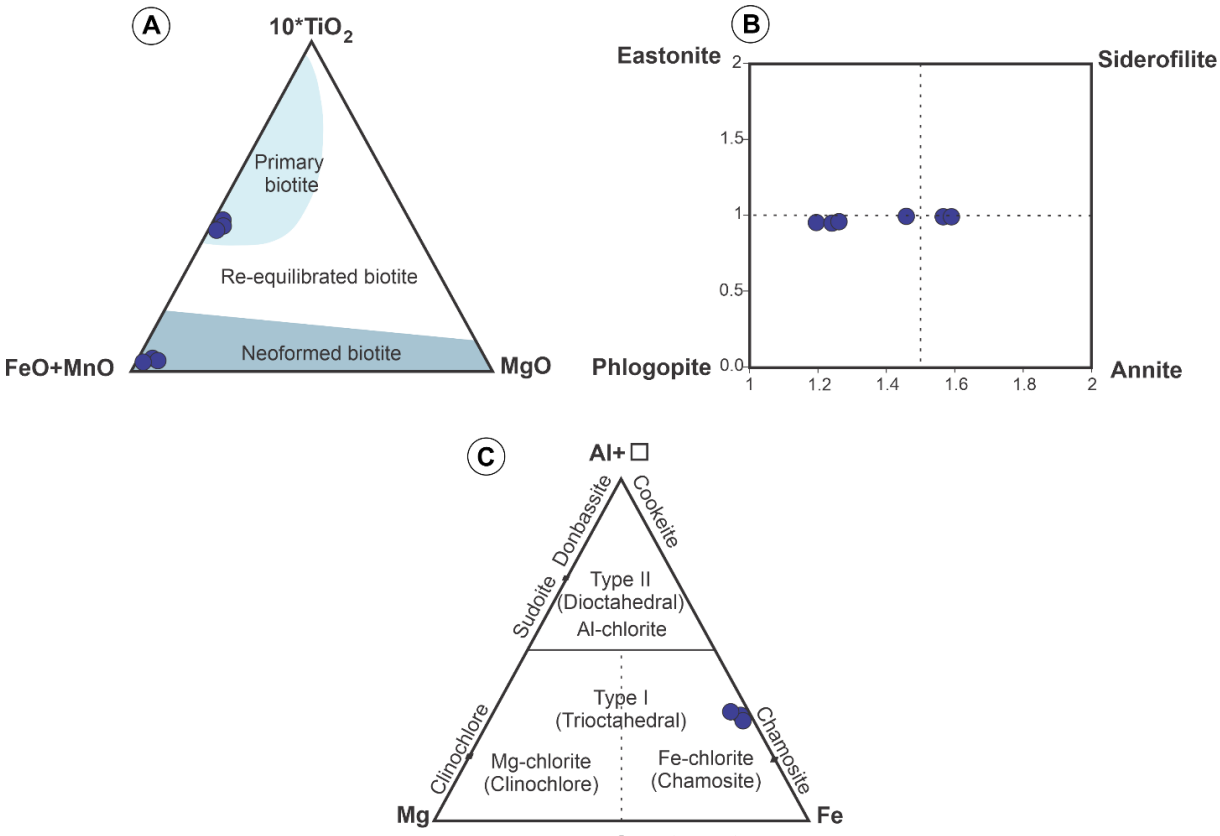


**Source:** Author (2022).

**Tabela 1 -** Representative electron microprobe analyses (wt. %) of feldspar in the metarhyolite samples.

| Mineral | Fds | Fds | Fds | Fds | Fds | Fds | Fds |
|---|---|---|---|---|---|---|---|
| Sample | P5 | P5 | P6 | P6 | P5 | P5 | P5 |
| Analysis | Q4-Kf1 | Q4-Kf2 | Qz6-Kf1 | Qz6-Kf2 | Q3-Kf1 | Q3-Kf2 | Q3-Kf3 |
| $SiO_2$ | 64.06 | 64.13 | 66.00 | 65.38 | 64.62 | 64.09 | 64.09 |
| $Al_2O_3$ | 17.55 | 17.55 | 18.72 | 18.40 | 18.42 | 18.42 | 18.70 |
| FeO | 0.25 | 0.23 | 0.04 | 0.06 | 0.01 | 0.01 | 0.06 |
| CaO | 0.03 | 0.01 | n.d | n.d | n.d | n.d | n.d |
| $Na_2O$ | 0.33 | 0.24 | 3.41 | 0.18 | 0.39 | 0.39 | 0.22 |
| $K_2O$ | 16.98 | 17.01 | 11.58 | 16.95 | 16.60 | 16.60 | 16.90 |
| BaO | 0.22 | 0.05 | 0.06 | 0.09 | 0.06 | 0.06 | 0.21 |
| Sum | 99.47 | 99.22 | 99.81 | 101.06 | 100.10 | 99.55 | 100.18 |
| Si (apfu) | 3.00 | 3.01 | 3.00 | 3.00 | 2.99 | 2.98 | 2.97 |
| Al | 0.97 | 0.97 | 1.00 | 1.00 | 1.01 | 1.01 | 1.02 |
| Fe | 0.01 | 0.01 | 0.00 | 0.00 | 0.00 | 0.00 | 0.00 |
| Ca | 0.00 | 0.00 | 0.00 | 0.00 | 0.00 | 0.00 | 0.00 |
| Na | 0.03 | 0.02 | 0.30 | 0.02 | 0.04 | 0.04 | 0.02 |
| K | 1.02 | 1.02 | 0.67 | 0.99 | 0.98 | 0.99 | 1.00 |
| X | 1.06 | 1.05 | 0.98 | 1.01 | 1.02 | 1.02 | 1.03 |
| Z | 3.97 | 3.98 | 4.01 | 3.99 | 4.00 | 4.00 | 4.00 |
| Or | 97.00 | 97.90 | 69.10 | 98.40 | 96.60 | 96.60 | 98.10 |
| Ab | 2.90 | 2.10 | 30.90 | 1.60 | 3.40 | 3.40 | 1.90 |
| An | 0.10 | 0.00 | 0.00 | 0.00 | 0.00 | 0.00 | 0.00 |

Apfu: atoms per formula unit. The structural formula was calculated using 8 oxygens. n.d. = not determined.

**Tabela 2 -** Representative electron microprobe analyses (wt. %) of muscovite in the studied metarhyolite samples.

| Mineral | Ms | Ms | Ms | Ms | Ms | Ms |
|---|---|---|---|---|---|---|
| Sample | P5 | P5 | P5 | P5 | P5 | P5 |
| Analysis | Fd2-6 | Fd2-7 | Fd2-8 | Fd2-9 | Fd2-10 | Fd2-11 |
| $Na_2O$ | 1.34 | 0.15 | 0.11 | 0.08 | 0.18 | 0.15 |
| $SiO_2$ | 52.71 | 47.49 | 46.72 | 45.72 | 45.73 | 46.76 |
| MgO | 0.17 | 0.49 | 0.53 | 0.47 | 0.42 | 0.48 |
| $Al_2O_3$ | 18.02 | 29.49 | 28.37 | 28.86 | 28.48 | 28.94 |
| $K_2O$ | 10.66 | 10.18 | 10.24 | 10.36 | 10.29 | 9.71 |
| CaO | 0.24 | 0.00 | 0.02 | 0.02 | 0.00 | 0.01 |
| $TiO_2$ | 0.00 | 0.41 | 0.38 | 0.30 | 0.43 | 0.23 |
| $Cr_2O_3$ | n.d | n.d | n.d | n.d | n.d | n.d |
| MnO | 0.17 | 0.07 | 0.01 | 0.06 | 0.05 | 0.03 |
| FeO | 11.30 | 7.52 | 7.52 | 7.92 | 8.49 | 7.38 |
| Sum | 94.61 | 95.80 | 93.90 | 93.79 | 94.07 | 93.69 |
| Si (apfu) | 3.72 | 3,23 | 3.25 | 3.20 | 3.20 | 3.24 |
| Ti | 0.00 | 0.02 | 0.01 | 0.01 | 0.02 | 0.01 |
| $Al^{IV}$ | 0.27 | 0.76 | 0.74 | 0.79 | 0.79 | 0.75 |
| $Al^{VI}$ | 1.23 | 1.60 | 1.58 | 1.58 | 1.55 | 1.61 |
| Cr | 0.00 | 0.00 | 0.00 | 0.00 | 0.00 | 0.00 |
| Fe | 0.66 | 0.42 | 0.43 | 0.46 | 0.49 | 0.42 |
| Mg | 0.17 | 0.04 | 0.05 | 0.04 | 0.04 | 0.04 |
| Mn | 0.01 | 0.00 | 0.00 | 0.00 | 0.00 | 0.00 |
| Ca | 0.01 | 0.00 | 0.00 | 0.00 | 0.00 | 0.00 |
| Na | 0.18 | 0.01 | 0.01 | 0.01 | 0.02 | 0.02 |
| K | 0.92 | 0.88 | 0.90 | 0.92 | 0.91 | 0.86 |

Apfu: atoms per formula unit. n.d. = not determined.

**Tabela 3 -** Representative electron microprobe analyses (wt. %) of biotite in the studied metarhyolite samples.

| Mineral | Bt | Bt | Bts | Bt | Bt | Bt |
|---|---|---|---|---|---|---|
| Sample | P5 | P5 | P5 | P5 | P5 | P5 |
| Analysis | Qz-Bt1 | Qz-Bt2 | Qz-Bt3 | Fd2-3 | Fd2-4 | Fd2-6 |
| $Na_2O$ | 0.11 | 0.04 | 0.10 | 0.07 | 0.08 | 0.11 |
| $SiO_2$ | 35.54 | 33.30 | 33.41 | 25.53 | 25.53 | 27.17 |
| MgO | 0.90 | 0.94 | 0.90 | 0.34 | 0.37 | 0.27 |
| $Al_2O_3$ | 15.47 | 15.23 | 16.12 | 14.60 | 14.78 | 13.98 |
| $K_2O$ | 9.52 | 9.52 | 9.60 | 0.20 | 0.26 | 0.43 |
| CaO | 0.02 | 0.00 | 0.02 | 0.54 | 0.55 | 0.70 |
| $TiO_2$ | 2.73 | 2.75 | 2.83 | 0.03 | 0.03 | 0.03 |
| $Cr_2O_3$ | 0.02 | n.d | 0.00 | 0.00 | 0.00 | n.d |
| MnO | 0.18 | 0.17 | 0.16 | 0.05 | 0.50 | 0.98 |
| FeO | 34.75 | 33.02 | 32.06 | 44.46 | 44.12 | 43.24 |
| Sum | 99.24 | 94.97 | 95.20 | 86.27 | 86.43 | 86.91 |
| Si (apfu) | 2.80 | 2.75 | 2.74 | 2.42 | 2.43 | 2.54 |
| Ti | 0.16 | 0.17 | 0.17 | 0.00 | 0.00 | 0.00 |
| $Al^{IV}$ | 1.19 | 1.24 | 1.25 | 1.57 | 1.56 | 1.45 |
| $Al^{VI}$ | 0.24 | 0.24 | 0.29 | 0.05 | 0.08 | 0.08 |
| Cr | 0.00 | 0.00 | 0.00 | 0.00 | 0.00 | 0.00 |
| Fe | 2.29 | 2.28 | 2.19 | 3.53 | 3.48 | 3.38 |
| Mg | 0.10 | 0.11 | 0.11 | 0.04 | 0.05 | 0.03 |
| Mn | 0.01 | 0.01 | 0.01 | 0.04 | 0.04 | 0.07 |
| Ca | 0.00 | 0.00 | 0.00 | 0.05 | 0.05 | 0.07 |
| Na | 0.01 | 0.00 | 0.01 | 0.01 | 0.01 | 0.01 |
| K | 0.95 | 1.00 | 1.00 | 0.02 | 0.03 | 0.05 |

Apfu: atoms per formula unit. n.d. = not determined.

## 5 DISCUSSION

All the studied metavolcanic rocks from the Novo Horizonte Formation exhibit similar chemical and petrographical data. The identified mineral assemblage fits with common acid

effusive rocks, reflecting the original magmatic composition, composed of quartz, K-feldspar, plagioclase, biotite, muscovite, fluorite, allanite, rutile, zircon, opaque minerals (mostly magnetite and hematite), and secondary phases, including carbonate, sericite, chlorite and phengite. However, evidence for later ductile deformation is present, interpreted as the result of tectonic inventions of the Brasiliano Orogeny (e.g., Brito Neves *et al*., 2014).

The samples show mineralogy and mineral chemistry typical of strongly peraluminous and alkaline magmas, common in anorogenic settings (Abdel-Rahman1994), and typical of blue quartz host rocks (Zolensky *et al*., 1988). The observed igneous paragenesis fits with the previous whole-rock geochemical interpretations of the Rio dos Remédios metavolcanic rocks association (e.g., Teixeira2005; Guimarães *et al*., 2008; Santos *et al*., 2019). Such an inference is strongly based on the observed equilibrium paragenesis of the muscovite-biotite pair, a trustful petrological indicator of magma composition (Abdel-Rahman, 1994).

Despite the primary mineralogy present in those samples, one must consider the role of metasomatic and deformational processes of variable crustal regimes, as attested by the extremely fractured, recrystallized, and altered crystals, as well as the widespread evidence for the formation of sericite and carbonate veins. We interpreted these events as coeval to the regional ductile deformation, possibly triggered by the migration of fluids in an intercrystalline form, destabilizing lesser phases (Santos *et al*., 2019), as evidenced by the described microstructures.

Rounded and embayed quartz phenocrysts, usually referred to as “quartz eyes,” occur in association with processes correlated to crystallization at high temperature, crystallization in a magmatic-hydrothermal system, disaggregation, and recrystallization of early quartz-rich bodies (Betsi and Lentz, 2010).

However, during deformation, conditions of reduction of elastic distortional energy, which occurs by the concentration of dislocation into walls, are driven to subgrain rotation. Thus, the crystal reaches extinction at slightly different angles, proving a mottled appearance, and there is the formation of small new grains, which are consistent with the deformation of preexisting phenocrysts (Guillope and Poirier, 1979).

The presence of K-feldspar megacrysts is associated with the relatively small amount of calcic plagioclase and mafic components in metaluminous and peraluminous granitoid systems, suggesting that a large amount of liquid is still available when K-feldspar begins to crystallize (Vernon, 1986). According to Winkler and Schultes (1982), about 60–70 wt.% of the liquid remains when K-feldspar starts to precipitate. Early crystallization of lesser amounts of mafic minerals, plagioclase, and quartz might take place; in this case, the

abundance of silica in the magma provides a high probability for the formation of large, ovoid to lenticular quartz phenocrysts.

When K-feldspar grows rapidly, there is plenty of space for them to expand, move, or incorporate other small phenocrysts. Thus, early crystallization of K-feldspar does not constitute the only explanation to form the megacrysts, since their formation is supposed to be part of a solid state, since the only requirement is enough to melt (30–40% at least; Vernon, 1986). On the contrary, the groundmass tends to deform relative to the phenocrysts, due to its fine grain size and composition (Vernon, 1986). Those characteristics are consistent with the deformation of the matrix containing preexisting large grains (Bradley, 1957).

The hydrothermal processes are well marked on biotite crystals since their cleavage planes enable the percolation of hydrothermal fluids. For instance, its Ti content is commonly controlled thermally; therefore, re-equilibrated and neo formed biotite lamellae might represent low-temperature hydrothermal reactions, which are characterized by low contents of Ti, as characterized by the group II biotites of the Novo Horizonte metarhyolite (Zhang *et al*., 2016). The formation of chlorite might also be interpreted as a fluid-rock reaction process, which is generally controlled by the reaction kinetics (Zhang *et al*., 2007). The chloritization of Novo Horizonte metarhyolites occurs when biotite is partially metasomatized, leading to chlorite growth. In addition, the chemical composition of chlorite crystals indicates that the fluids are rich in Fe or that they might have been able to extract Fe components of the host rock during metasomatic events. Thus, the formation of chlorite could be associated with dissolution-precipitation mechanisms, manifested by hydrothermal fluid metasomatized biotite (Zhang *et al.*, 2006; Wu *et al*., 2019).

The abundance of albite revealed by the XRD analysis could also be explained by the presence of late metasomatic fluids, forming intergrowths of albite in K-feldspar and granophyric texture of quartz in K-feldspar. According to Barker and Burmester (1970) and Cox *et al*. (1979), granophyric textures usually result from a silicate melt at the eutectic point, r in the presence of a water-rich phase, when the magma is significantly undercooled. Allanite could also have been introduced into the system by rare earth element-bearing fluids (Gros *et al*., 2020).

The combination of field relationships, mineral assemblage and chemistry of these rocks is in accordance with an intraplate environment, associated with the continental rift of the Chapada Diamantina. Rhyolite origin in intraplate continental settings is strongly related to the interaction of primary mafic magma with the surrounding crust, at crustal depths (Halder et al.2021). The partial melting of an underplated mantle, with the intrusion of crustal

material triggering hydrothermal reactions, is a good model to explain the origin of the Rio dos Remédios metarhyolites.

## 6 CONCLUSION

The metarhyolites from the Novo Horizonte Formation show a characteristic mineral assemblage formed by quartz, K-feldspar, biotite, muscovite, zircon, ilmenite and rutile. High silica and peraluminous metarhyolites show transitional magmatic affinities and intraplate crustal-derived A-type signatures.

The mineral assemblage exhibits feature of deformational and associated hydrothermal alteration. The hydrothermal processes are marked by the complete or partial replacement of some mineral phases (biotite, K-feldspar) forming secondary assemblages, mainly represented by chlorite, sericite, phengite and carbonate. The compositional differences of biotite types and the presence of allanite are also great evidence of fluid action.

Deformational effect is well marked by the abutment of groundmass foliation against phenocrysts, rather than deflection around them. Due to the presence of megacrysts, the fine-grained, polymineralic aggregates of the matrix have the tendency to undergo deformation (Vernon, 1986).

Despite the alteration on these rocks, the East portion of the body was more affected, forming garnet, andalusite and kyanite phases (Santos *et al*., 2019). Therefore, the Paramirim portion would be a better representative of the primary features of the Rio dos Remédios Group. Nevertheless, the characterization of these processes is challenging due to the Brasiliano overprinting.

## ACKNOWLEDGMENTS

This work is part of the first author's MSc dissertation, which has been supported by grants provided by the Universidade Federal de Permambuco and the Instituto Nacional de Ciência e Tecnologia (INCT) para Estudos Tectônicos. We are indebted to the Conselho Nacional de Desenvolvimento Científico e Tecnológico (CNPq) of Brazil for the first author's scholarship. We also thank the Microscopy and Microanalysis Laboratory of the Universidade Federal de Ouro Preto, a member of the Fundação de Amparo à Pesquisa do Estados de Minas Gerais (FAPEMIG). L. Montefalco and G. Queiroga are fellows of the Brazilian Research Council (CNPq) and acknowledge the support given. We would like to express our gratitude to Prof.

Pedro Luiz Guzzo (UFPE) for the x-ray analysis performed at the Laboratório de Tecnologia Mineral (LTM) as well as his contributions on the manuscript.

# 3 MULTI-ANALYTICAL STUDY OF DISTINCTIVE PROPERTIES OF ROCK-FORMING BLUE QUARTZ: RIO DOS REMÉDIOS GROUP, PARAMIRIM AULACHOGEN, NE BRAZIL OCCURRENCE

Danielle Cruz da Silva[1]*, Pedro Luiz Guzzo[2]; Lauro Cézar Montefalco de Lira Santos[1], Glaúcia Queiroga[3]; Mahyra Ferreira Tedeschi[4]

[1]Departamento de Geologia, Universidade Federal de Pernambuco, Av. da Arquitetura, Cidade Universitária, 50740-540, Recife, Pernambuco, Brazil
[2]Departamento de Engenharia de Minas, Universidade Federal de Pernambuco, Av. da Arquitetura, Cidade Universitária, 50740-540, Recife, Pernambuco, Brazil
[3]Departamento de Geologia, Escola de Minas, Universidade Federal de Ouro Preto, Morro do Cruzeiro, 35400-000 Ouro Petro, Minas Gerais, Brazil
[4]Instituto de Geociências, Universidade Federal de Minas Gerais, Av. Antônio Carlos, 6627, Belo Horizonte, Minas Gerais, Brazil

**Corresponding author. e-mail: dani.cs8@live.com*

**ABSTRACT**

Blue quartz is a rare component of igneous rocks but occurs in a different type of felsic rocks and their metamorphosed equivalents. Blue quartz grains usually present as rock-forming $SiO_2$ phenocrysts and contain high concentrations of submicron-sized solid inclusions. Since the pioneering study of Indings (1904), 245 occurrences are known around the world, and 19 of them are located in Brazil. The Rio dos Remédios occurrence is one of the meaningful representations in Brazil, but besides the numerous studies of the color, the literature is still poor, and its origins remains controversial. The blue quartz from the Rio dos Remédios metavolcanic rocks contains significant amounts of submicrometer-sized rutile inclusions, possibly originated by epigenetic exsolution of Ti. The presence of these inclusions probably drives the scattering of light (Rayleigh scattering), that best explains the origin of the blue color. The blue quartz bearing-rocks are generally Ti-rich and formed by alkaline magma compositions (A-type). Although it is accepted that the origin of the inclusions is strongly associated with the magma characteristics (High Ti and Fe contents, high temperature and alkaline caractherists), the geological significance remains undetermined.

**Keywords:** Blue quartz. Inclusions. Exsolution. Submicron inclusions. Ti-rich rocks.

## 1 INTRODUCTION

Quartz and its varieties occupy a significant fraction of the earth's continental lithosphere, occurring in abundance in various common crustal rocks, such as granites, rhyolites, gneisses, and sedimentary siliciclastic rocks. Although colorless in its most common form, quartz's visual appearance might reflect the conditions under which it was formed, exhibiting a large number of colored varieties of economic importance such as amethyst, citrine and aventurine.

Blue colored quartz crystals are rare components in igneous rocks, occurring mainly in felsic rocks such as granites, granodiorites, rhyolites, charnockites, that are mostly crystallized in within-plate settings (Zolensky *et al*., 1988), also including their metamorphic equivalents (Seifert *et al*., 2011). The occurrence of blue quartz in plutonic-volcanic systems is frequently associated with nanometer size mineral inclusions that are capable of producing the color through the Rayleigh scattering of light (e.g., Zolenski *et al*., 1988; Heinrich, 2014).

Detailed descriptions of blue-quartz-bearing rocks was firstly made by by Iddings (1904), who studied the unique occurrence of the rhyolite rocks of the Llano Uplift (Texas), making it the most famous and best studied occurrences of blue quartz in the world. A total of 245 occurrences of blue quartz are known worldwide, related crustal segments of all ages (Pantia *et al*., 2019). In Brazil, 19 occurrences are documented, including those related to the Porangatu Granulitic Complex, the Lagoa Real subalkaline granitic domain, in central Brazil and the Enseada dos Zimbros dyke swarm in Southern Brazil. In addition, the Bahia state in NE Brazil became famous over the last decades, due to the concentration of the most significant occurrences that have the potential to become an indicator for metamorphic/tectonic conditions for blue quartz bearing volcanic rocks crystallization (*e.g.*, Cruz da Silva *et al*., 2023; Pantia *et al.*, 2022).

In the region, one of the most famous occurrences is part of the Rio dos Remédios Group (RR), of the São Francisco Craton, East-central Bahia State. Associated blue quartz-bearing rocks include acid to intermediate metavolcanic rocks that crop out interleaved with pyroclastic and quartzites (Arcanjo *et al*., 1999).

Despite the number of worldwide occurrences, the study of the presence of blue quartz in rocks in the Brazilian territory is practically absent, except from punctual contributions (*e.g.*, Arancajo, 1999; Rosa, 1999; Craveiro *et al.*, 2019). In this paper, we aim to procedure a

multi-analytical study of the blue quartz occurrence from the Rio dos Remédios Group in order to investigate their main morphological and chemical aspects as well as discuss the role of mineral inclusions that might provide glimpses on the origin of quartz coloration of these rocks.

## 2 GEOLOGICAL SETTING

The studied occurrences are located on the morphotectonic domain of the Paramirim Aulacogen, Northern portion of the São Francisco Craton (Fig. 11). This aulacogen represents an NNW intracontinental rift system developed from a succession of syneccleses starting at ca. 1.70 and being later inverted at *ca.* 0.65 Ga during the Brasiliano orogenic cycle (Alkmin *et al*., 2007; Santana, 2016; Cruz; Alkmin, 2017).

Its geological framework comprises two major lithostratigraphic units: i) the Espinhaço Supergroup (Schobbenhaus, 1996) and ii) the São Francisco Supergroup (Cruz *et al*., 2007). Both successions were strongly deformed due to the number of tectonic inversions that took place during the Late Neoproterozoic (ca. 0.6 Ga; Guimarães *et al*. 2005; 2012; Guadgnin and Chemale Jr., 2015; Cruz and Alkmim, 2017; Danderfer Filho, 2000).

The study rocks are part of the Rio dos Remedios Group, a regional-scale unit of the Espinhaço Supergroup. It is interpreted as a metavolcanosedimentary sequence of dominant sedimentary terrigenous protoliths that are interleaved with the studied blue-quartz bearing acid to intermediate metavolcanic rocks, mainly at its basal portion (*e.g.*, Cruz *et al*., 2007; Medeiros, 2013).

**Figura 1** - Map of the São Francisco Craton showing the bordering Neoproterozoic Brasiliano belts, the morphotectonic domain of the Paramirim aulacogen and the proterozoic cover sequence (younger than 1.8 Ga) of the Espinhaço Supergroup.

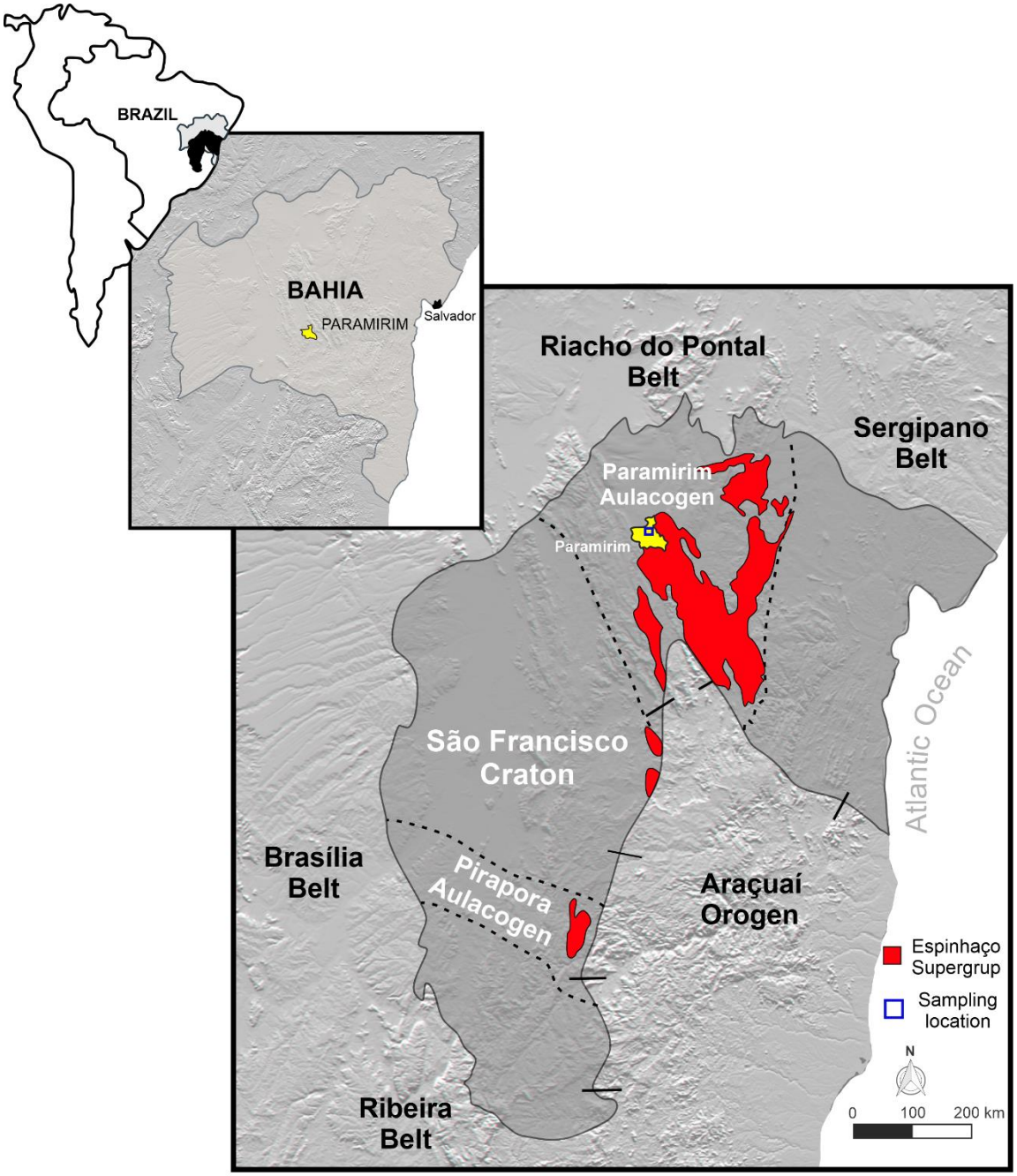


**Source:** Modified from Alkmin *et al*. (2007).

In the Paramirim region, only volcanic members of the Rio dos Remédios Group crop out (Fig. 12). They correspond to metamorphosed porphyrytic dacites, rhyolites and andesites, moderately deformed by local ductile shear zones (Barbosa, 2012; Danderfer and Dardenne,

2002; Santos, 2019). The metavolcanic rocks crop out as 2-10 dimensions-long blocks and boulders of dominant greyish colors, exhibiting mesoscopic porphyritic texture and marked by feldspar and blue quartz asymmetrically deformed phenocrysts (Fig. 13).

**Figura 2 -** Geological map of the Espinhaço Supergroup, highlighting the Southeast of Bahia region, the Rio dos Remédios Group and sampling location (Cruz da Silva *et al*., 2023).

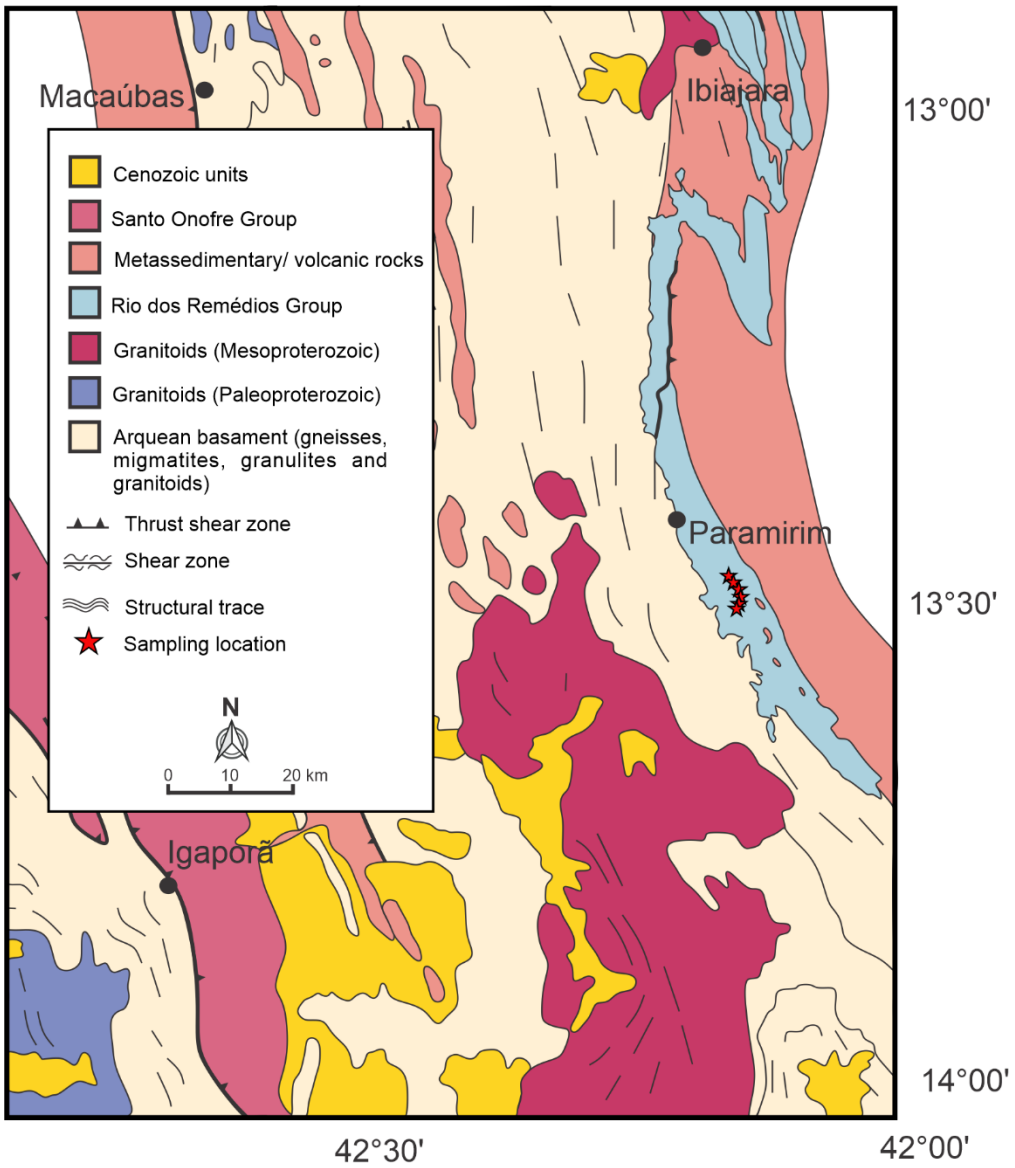


**Source:** Cruz da Silva *et al*. (2023).

**Figura 3 -** Field and macroscopic aspects of the Rio dos Remédios rhyolites. Rocks from the Rio dos Remédios Group exposed as (A) rhyolitc layers and (B) as massive blocks. (C) Porphyritic texture with blue quartz and k-feldspar phenocrysts. (D) Features of the felsitic ground mass and caractheristics of the K-feldspar phenocrysts, clusters of parallel crystals.

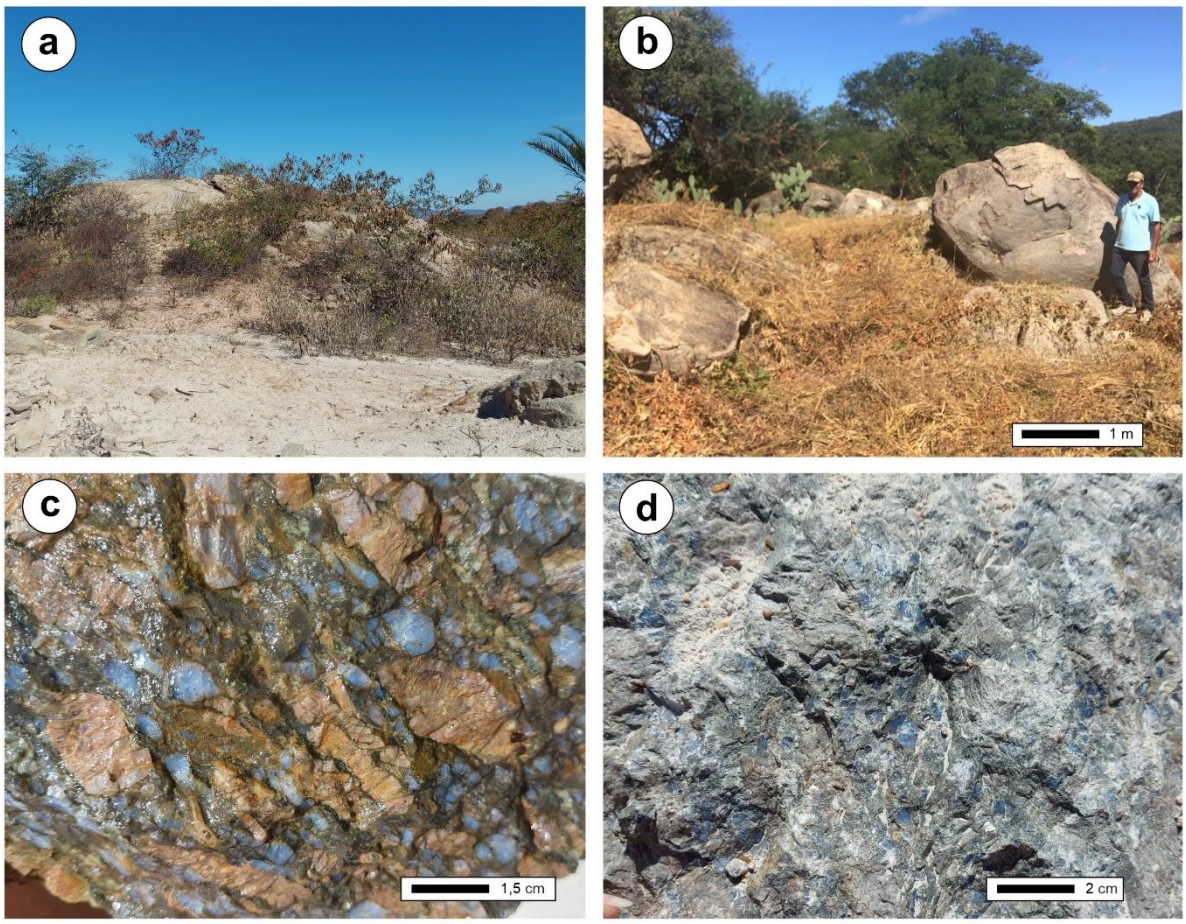


**Source:** Author (2023).

## 3 ANALYTICAL INSTRUMENTATION AND METHODS

### *Sample selection and thin section preparation*

Fifteen representative samples collected at Paramirin town (geographical coordinates -13.52443, -42.17279) were selected for petrographic studies and four of them chosen (since they best represent the collected samples) for, scanning electron microscope (SEM) analyzes as well as electron microprobe (EPMA), Raman, IR spectroscopy, transmission electron microscope (TEM) and X-ray diffraction (XRD) studies.

The samples were prepared in two different ways: common thin sections and bi-polished sections. Thin section preparation was performed at the Laboratório de Gemologia at

the Universidade Federal de Pernambuco, Brazil. The samples were cut in the approximate dimensions of 35 x 20 mm on the MultiMachine Lapidary Saw. After cutting, the samples were bonded with epoxy to and then cut again with a Labcut 1010 precision saw and ground on polished at Arapol VV. The final polishing was performed with diamond solution in suspension at granulations 1 μm and 3 μm on flocked velvet cloth (FVL), resulting in thin sections of approximately 300 μm thick. The final samples were used to carry out analyzes in optical microscopy, scanning electron microscopy (SEM), electron probe microanalysis (EPMA), transmission electron microscope (TEM) and Raman.

The bi-polished slabs were prepared at the Laboratório de Tecnologia Mineral of the Universidade Federal de Pernambuco, for IR spectroscopy. The material was cut with a diamond saw in slabs of 3.0-3.5 mm thickness, with dimensions of 1 x 1 cm approximately, in two different crystal directions, parallel and perpendicular to the thin section samples. The faces of each slab were lapped with alumina increasing grit size (200, 400, 600, 800, 1000 and 2000) and then optically polished with alumina suspension (1 and 2 μm), achieving the desired thickness of 1.1 mm.

***Single grain preparation, size and morphology analysis***

The selected crystals extracted from the four samples were cleaned with alcohol and acetone, followed by hydrofluoric acid and a solution with 15% hydrochloric acid diluted in water, 15 min each. After a superficial cleaning, the material was kept in a 10% hydrochloric acid solution for 72 hours.

The resulting materials were granulometric analyzed using a set of sieves with openings, in mm, of 4750x3350, 3350x2360, 2360x2000 and 2000x1700. The crystals were scanned by size, using a multifunctional Epson Stylus TX135. The CuverMeter plugin was used to extract 2D variables that include the perimeter (P), area (A), and width (W). The shape parameters, elongation, and circularity, of the crystals were analyzed following the methodology proposed by Hemmati *et al*. (2020), which uses data referring to the area, perimeter, and width to perform the characterization of the crystals through mathematical analysis (see Fig. 14).

**Figura 4 -** Representation of the geometric features measured in this study, length, width, the smallest circumscribed circle and the smallest circumscribed rectangle and the mathematical formulas.

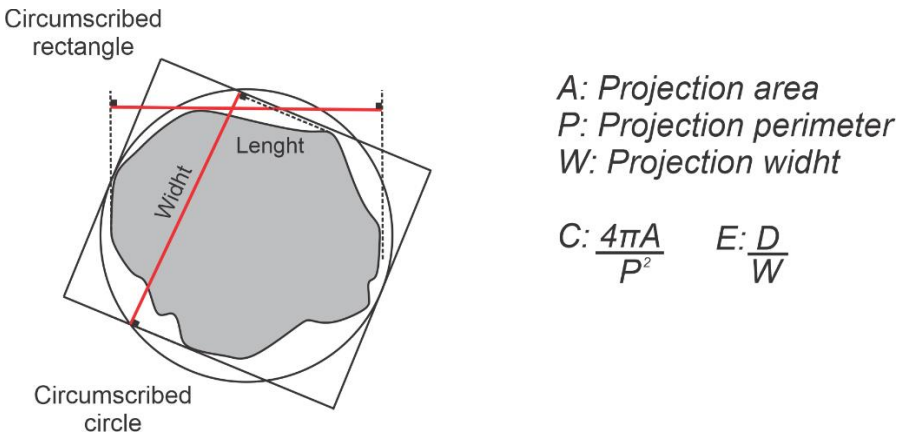


**Source:** Hemati *et al*. (2020).

***Imaging and trace elements analysis***

Scanning Electron Microscopy analyzes were performed at the Laboratório de Micropaleontologia Aplicada at the Universidade Federal de Pernambuco. The analysis of the four selected thin sections were carried out using a Phenom 167XL with a backscattered electron detector (BSE). The generator voltage, radiation and current were fixed at 15 kV.

The EPMA analyzes were accomplished using a JEOLJXA8230 instrument in the Labororatório de Microscopia e Microanálises (LMIc) at the Universidade Federal de Ouro Preto, Brazil. The analyzes were conducted at 15kV acceleration voltages, current of 20nA, and spot sizes of 5-10 μm. The natural standards used on the instrument were: Si (quartz), Na (anorthoclase), K (microcline), Mn ($MnO_2$), Mg (olivine), Ca (fluorapatite), P (fluorapatite), Al (corundum), Fe (metallic Fe), F ($CaF_2$), Cl (scapolite), Ba ($BaSO_4$), Cr (chromite), Sr (strontianite), Ti (rutile) and Zn (gahnite). Counting times on the peaks and background were 10 and 5 s for all the elements. Matrix corrections of common ZAF (atomic number, absorption, fluorescence) were applied.

TEM was performed at the Materials and Transformations Unit of the University of Lille, France. The analyzes were carried out using two microscopes, one FEI® Tecnai G2-20 model operating at 200 kV and a Philips CM30 microscope operating at 300 kV, both equipped with LaB6 filament and using a double inclination sample holder. Automated crystal orientation mapping (ACOM-TEM) was performed in the TEM with the ASTARTM tool from NanoMEGAS.

### *X-ray diffraction*

The X-ray diffraction (XRD) measurements were conducted at the Laboratório de Tecnologia Mineral of the Universidade Federal de Pernambuco, with two different powdered samples: whole rock and single crystals. Both analyses were performed on a Bruker D2 PHASER using Cu-Kα radiation equipped with a Bruker-AXS-Lynxeye detector. The voltage, radiation and current of the generator were set at 40 kV, 1.54060 Å and 20 mA (P = 300W) respectively. The diffraction pattern was recorded for 2θ from 5º to 80º with step scan of 0.02019º in a constant rotation of 10 rpm, counting for 1.5 s at every step. The results were indexed using the app DIFFRAC.EVA with the database COD (REV212673 2018.12.20).

### *Spectroscopy analysis*

IR spectroscopy was carried out at the Laboratório de Tecnologia Mineral of Universidade Federal de Pernambuco. The experiments were carried out using a double-beam UV-Vis spectrometer, model Lambda 35 by Perkin Elmer. Scanning was at 120 nm/min, non-polarized light beam and wavelength varying between 190 and 1100 nm. The slit aperture used was 4 nm.

The Raman analyses were performed in the Laboratório de Espectroscopia Raman, at the Universidade Federal de Minas Gerais, Brazil, on a HORIBA LabRAM HR Evolution, equipped with charge-coupled device (CCD) detector and with 600g/mm diffraction grating, giving spectral resolution better than $2cm^{-1}$. The Raman spectra of the selected sections were acquired integrating 2-10 repetitions of 20-10s, using a red-light laser of 632 nm and collected by the software Labspec6 (Horiba Scientific). All the measurements were conducted in the backscattering geometry under room-temperature conditions. The samples were focused by a 50x objective (NA=0.55) and the laser power at the sample surface was kept below 1mW to avoid sample heating. The mineral identification was conducted by comparing the acquired data spectra with those reported by RRUFF database and Frezzotti *et al*. (2012).

## 4 RESULTS

### *Petrography*

The optical microscopy carried with crossed polarizes light in several sections of parent samples indicated the presence of secondary mineralogy composed by sericite, fluorite, allanite, sericite and carbonate. Microscopically the metarhyolites exhibit a grayish color and 1-3 cm long quartz and feldspar phenocrysts, surrounded by a fine-grained leucocratic

groundmass, composed of the primary and secondary mineralogy. In thin sections the phenocrysts may preserve their primary crystalline habits, except for the most deformed samples. However, those of the fin-grained matrix are always strongly deformed and fractured, characteristic of deformation and hydrothermally effects.

Quartz crystals including the blueish varieties occur with subhedral to anhedral shapes, including well-developed porphyroclasts and as part of fine-grained groundmass. The larger crystals exhibit rounded to subrounded shapes, also including engulfment and magmatic corrosion textures (Fig. 15a).

Feldspar phenocrysts are up 4mm and exhibit subhedral to anhedral shapes, including and tabular and sigmoidal habits. The crystals show flow orientation marked by the alignment of eye-shaped crystals and form clusters aligned with widespread minor-sized grain aggregates (Fig. 15b and 15c).

Muscovite occurs as very thin lamellae forming oriented clusters along the matrix or surrounding the phenocrysts (Fig. 15d). Biotite exhibit subhedral to anhedral habits, light brown colors. They form bent-flake lamellae aggregates. Sometime occurs associated to fluorite, chlorite and sericite (Fig. 15e). The main opaque minerals are magnetite, ilmenite, rutile and minor unidentified iron-oxides, allanite occurs associated to these minerals (Fig. 15f).

**Figura 5 -** hotomicrographs with cross polarized of the samples of Rio dos Remédios metarhyolites. (a) Quartz (Qz) phenocrysts exhibiting rounded and engulfment shapes, undolose extinction and fractures. (b) Quartz “eyes” surrounded by muscovite (Ms) veins. (c) K-feldspar (Kfs) phenocryst and plagioclase (Pl) crystal with well-developed albite twinning. (d) Oriented muscovite veins and very altered K-feldspar crystals as part of the groundmass. (e) Biotite (Bt) and K-feldspar crystals strongly altered, forming aggregates of sericite (Ser) and fluorite (Fl). (f) Allanite (Al) crystals associated to Fe-Ti opaque minerals.

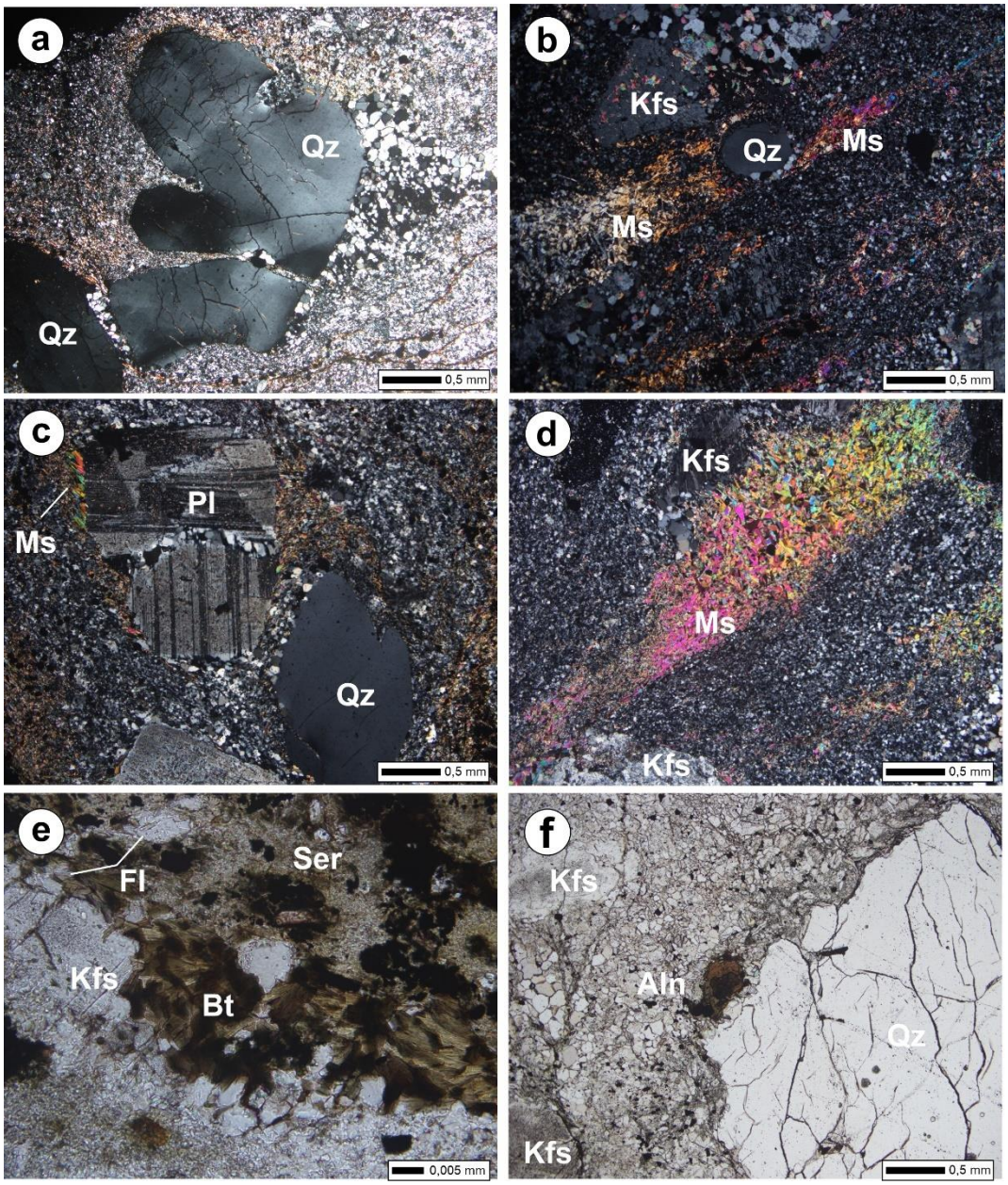


**Source:** Author (2023).

The whole-rocks XRD (Fig. 16) analyses enhance the mineralogical control of the samples. The mineralogical results obtained are concordant to the petrographic analysis (see Fig. 15). The indexed diffractograms exhibit quartz, albite, microcline, muscovite and biotite mineral phases as the main rock components.

**Figura 6 -** Representative diffractogram of the metarhyolites from Rio dos Remédios Group. The main mineral phases are quartz, microcline, albite, biotite and muscovite.

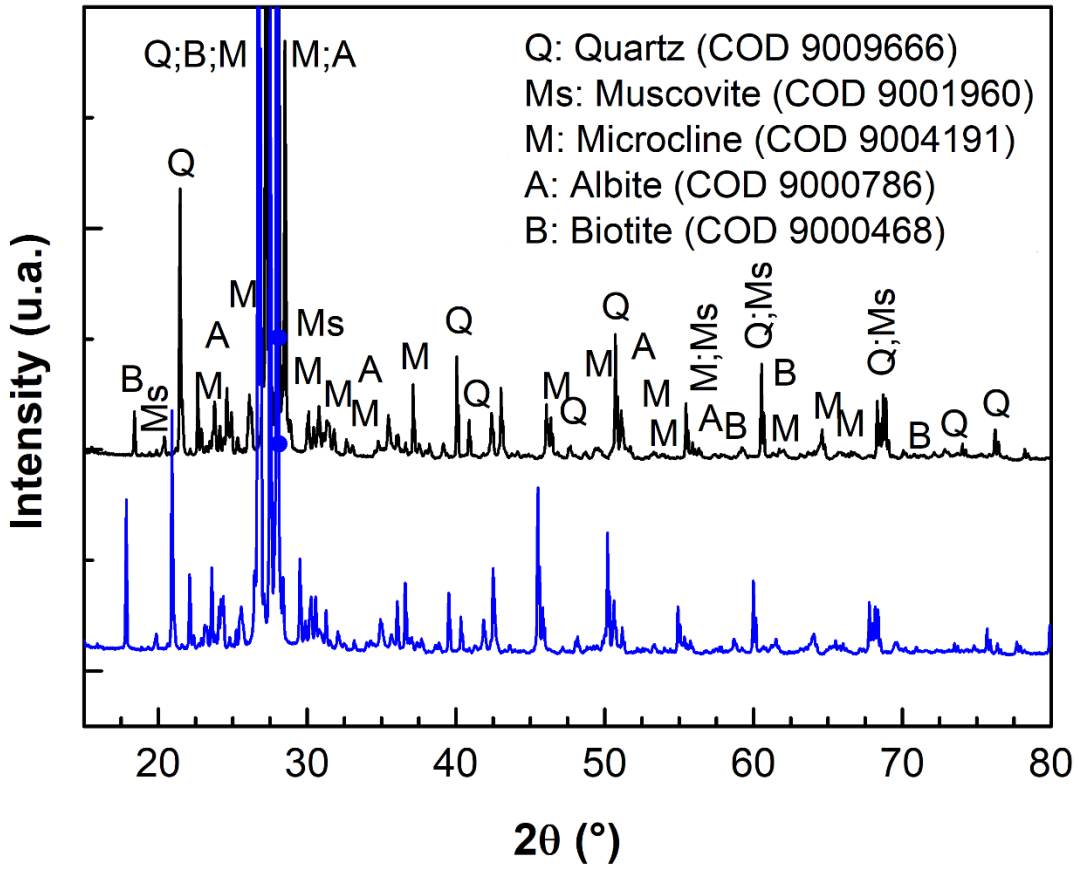


**Source:** Author (2023).

***Size and morphology of quartz grains***

Typical particle size distribution is shown in Fig.17. Most of the extracted grain particles are concentrated around 0.2 cm, the minimum ($d_{10}$) and maximum size ($d_{90}$) size for the particle were calculated and the results are around 1.5 cm and 3.2 cm each.

**Figura 7 -** Grain size distribution curves of retained fractions of blue quartz from Rio dos Remédios Group.

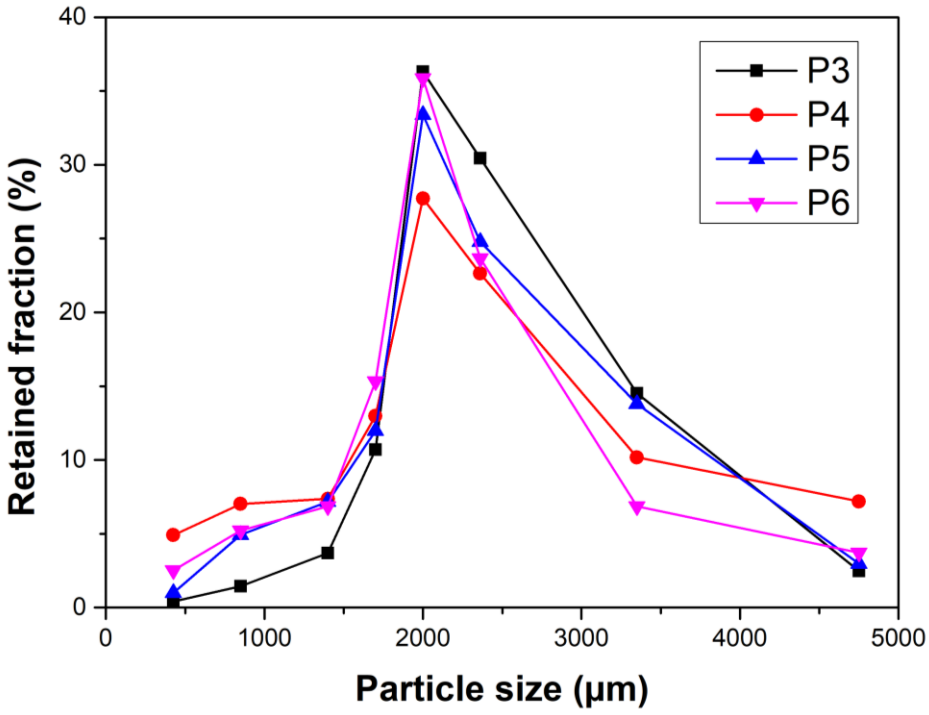


**Source:** Author (2023).

The quartz crystals from metavolcanic rocks of Rio dos Remédios Group show elongated, extremely fractured and slightly rounded shapes, similar to the observed in the petrography. These characteristics are present in Fig. 18, the color of the crystal is highly dependent on the background and the thickness of the samples, thus sometimes they do not show the blue color. The shape descriptors for the analyzed samples are displayed at Tab. 4. It is observed that the grain elongation and circularity show the same range of values for all the particles. Most of the edges are rounded and the crystals slightly elongated and do not show any visible inclusions.

**Figura 8 -** Reflect light images of the Rio dos Remédios blue quartz showing the color zoning observed and probably associated to different inclusion concentration inside the crystal.

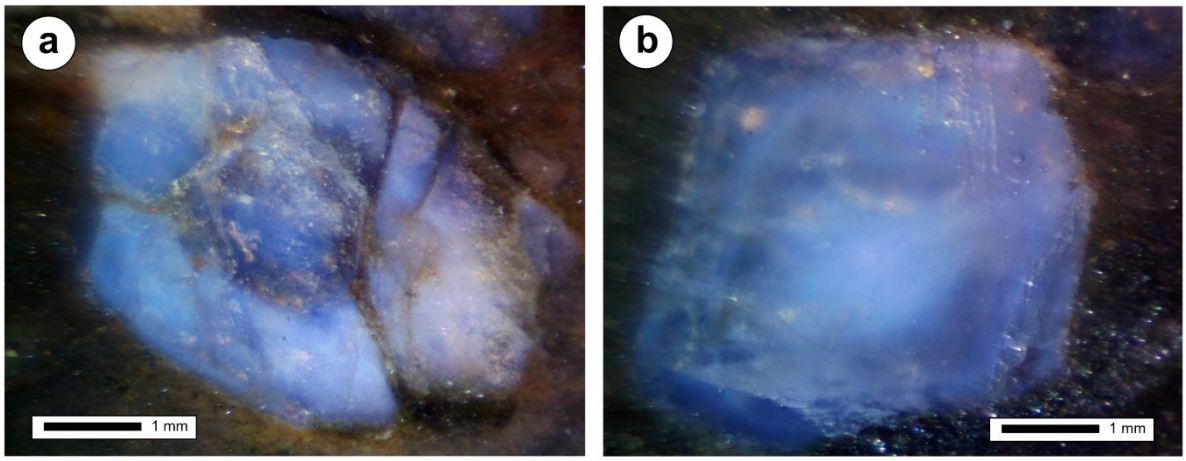


**Source:** Pantia, (2021).

**Tabela 1 -** Grain shape descriptors for the blue quartz crystals according to the grain size distribution.

| Size range (mm) | Elongation | Circularity |
|---|---|---|
| **4750x3350** | 1.28±0.05 | 0.87±0.21 |
| **3350x2360** | 1.36±0.21 | 0.86±0.07 |
| **2360x2000** | 1.38±0.31 | 0.85±0.07 |
| **2000x1700** | 1.42±0.32 | 0.84±0.07 |

**Source:** Author (2023).

### *Structural characterization of quartz crystals*

In the attempt to clarify the mineral identification, XRD was carried on powered quartz grains. The XRD analysis was carried out in two samples of quartz crystals, both corresponding to blue quartz, however with different intensities of color. The XRD patterns for two samples are shown in Fig. 19. The different samples exhibit the characteristic peaks of common quartz. It was not possible to identify any differences in the microstructural properties of the quartz crystals in both samples.

The IR spectra in Fig. 20a shows absorption bands at 3620, 3480, 3380, 2980, 2690 and 2595 $cm^{-1}$. According to Kats (1962), the band 3620 $cm^{-1}$ is associated to $K^+$ ions. The band 3480 $cm^{-1}$ corresponds to the O-H vibration due the $Li^+$ ions, and the band 3380 $cm^{-1}$ is associated with $[AlO_4/H]^0$ center (Kats, 1962; Guzzo *et al*., 2017). The sharp bands observed

at 2680 and 2595 $cm^{-1}$ are assigned to be SI-O overtones and the band 2690 is due to hydrogen vibration present during the experiment, as described by Kats (1962).

**Figura 9** - XRD partners showing the characteristics diffracting peaks for Rio dos Remédios blue quartz.

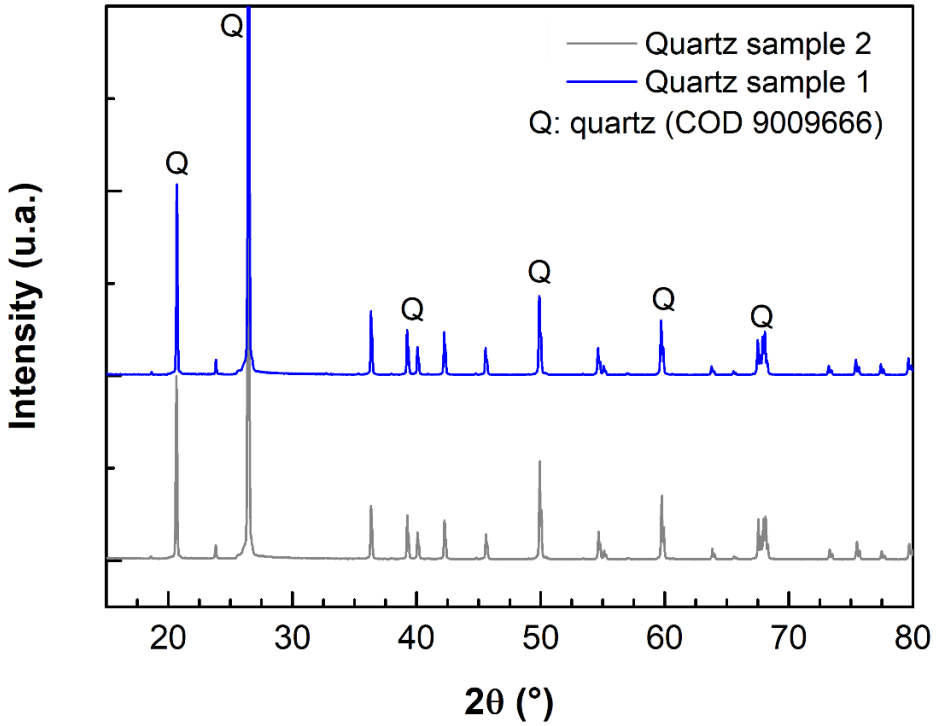


**Source:** Author (2023).

Raman spectroscopy provides a fast identification of individual minerals, due to their unique crystal lattices. However, the analyzed Raman spectra for the samples, as the XRD patterns, were not capable to identify easily any different mineral phases but resulted in a weak rutile-related spectrum (Fig. 20b). The mineral inclusions associated to the blue quartz range between 55 and 27 nm and the quartz bands are too strong, hiding the possible identification of minor inclusions presence.

**Figura 10 -** (a) IR spectra obtained at room temperature for blue quartz polished plates. (b) Raman spectra of standard quartz and mixed spectra of quartz and rutile.

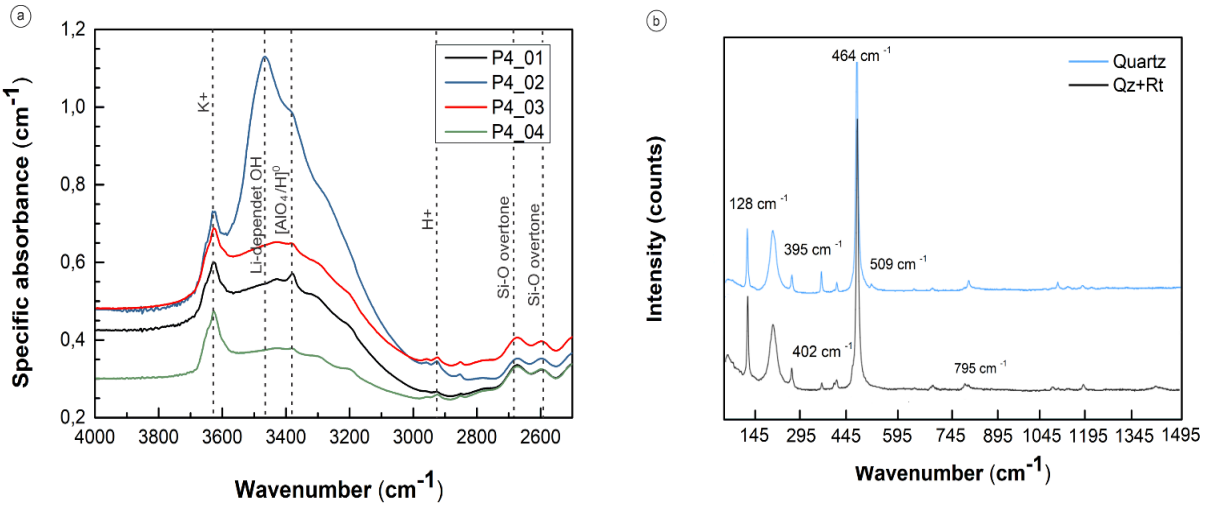


**Source:** Author (2023).

### *Major traces elements in quartz crystals*

The board present in Fig. 21 shows the concentration of the major and trace elements measured in blue quartz crystals. Ti is by far the major trace impurity present in all analyzed samples, followed by Fe, Na and K. Iron, aluminum and titanium are the main elements associated with blue quartz, where Ti concentrations range between ~11 and 100 ppm, normally >100 ppm. It was not possible to identify differences about the grain cores and rims. Al and Fe concentrations vary significantly in all samples, not showing a clear pattern, this could indicate that a major part of these elements is incorporated into the structure of the groundmass, as suggested by Seifert *et al*. (2011) measurements.

**Figura 11 -** Board of the r*esults of EPMA for blue quartz grains of Rio dos Remédios Group.*

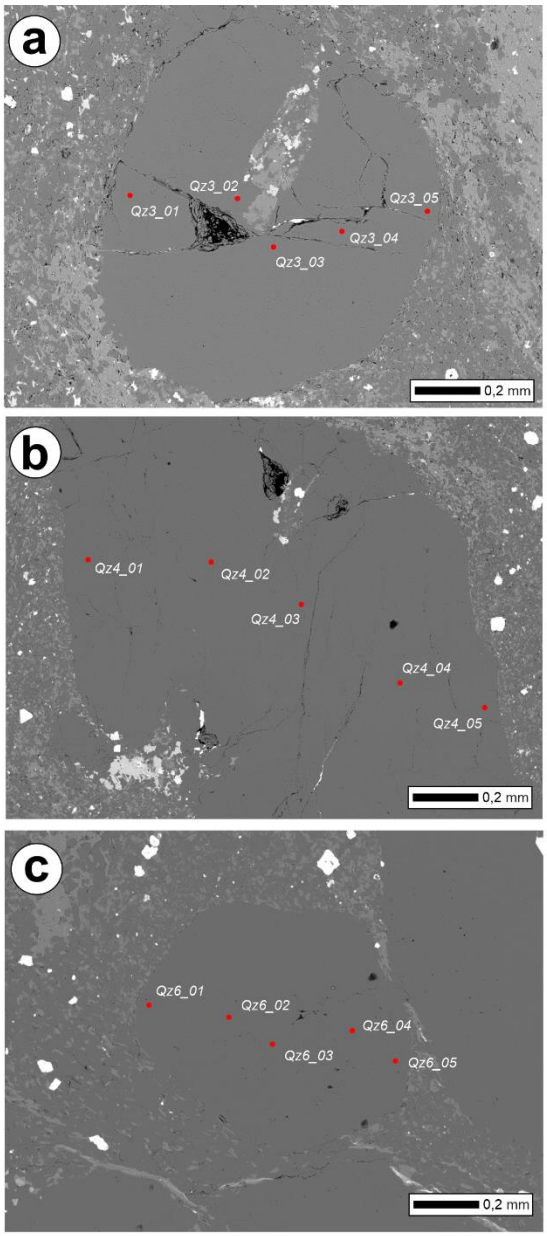


| Samples | Al | Na | K | F | Fe | Ti |
|---|---|---|---|---|---|---|
| Qz3_01 | 0.00 | 7.49 | 0.00 | 190.00 | 341.92 | 311.69 |
| Qz3_02 | 894.52 | 0.00 | 1021.02 | 370.00 | 3419.24 | 173.83 |
| Qz3_03 | 15.88 | 37.46 | 8.30 | 50.00 | 50.00 | 23.98 |
| Qz3_04 | 0.00 | 0.00 | 74.71 | 0.00 | 0.00 | 131.87 |
| Qz3_05 | 58.22 | 0.00 | 49.81 | 0.00 | 0.00 | 149.85 |

| Samples | Al | Na | K | F | Fe | Ti |
|---|---|---|---|---|---|---|
| Qz4_01 | 0.00 | 74.97 | 32.20 | 0.00 | 170.96 | 0.00 |
| Qz4_02 | 206.43 | 0.00 | 0.00 | 910.00 | 26.99 | 11.99 |
| Qz4_03 | 2011.72 | 29.96 | 132.82 | 0.00 | 0.00 | 203.80 |
| Qz4_04 | 5.29 | 0.00 | 16.60 | 0.00 | 0.00 | 293.71 |
| Qz4_05 | 0.00 | 14.98 | 33.20 | 0.00 | 62.99 | 131.87 |

| Samples | Al | Na | K | F | Fe | Ti |
|---|---|---|---|---|---|---|
| Qz6_01 | 47.64 | 44.95 | 99.61 | 400.00 | 386.91 | 191.81 |
| Qz6_02 | 0.00 | 74.91 | 0.00 | 0.00 | 0.00 | 167.83 |
| Qz6_03 | 0.00 | 119.86 | 116.21 | 210.00 | 9.00 | 269.73 |
| Qz6_04 | 0.00 | 0.00 | 66.41 | 0.00 | 9.00 | 35.96 |
| Qz6_05 | 74.10 | 232.22 | 0.00 | 0.00 | 350.92 | 203.80 |

**Source:** Author (2023).

### *Solid inclusions in quartz crystals*

Scanning electron microscopy images (Fig. 22), demonstrate the presence of solid inclusions in the blue quartz crystals. Oxides and zircon make up the majority of these inclusions. It was possible to analyze the inclusions and they show Fe/Ti compositions compatible with Ti-bearing oxides, such as ilmenite and rutile. These minerals usually appear as thin platy crystals.

**Figura 12 -** Scanning electron microscopy images of quartz inclusions present in the metarhyolites. Overview of quartz crystals and microinclusions of (a) zircon (Zr) and (b) Ilmenite (Ilm).

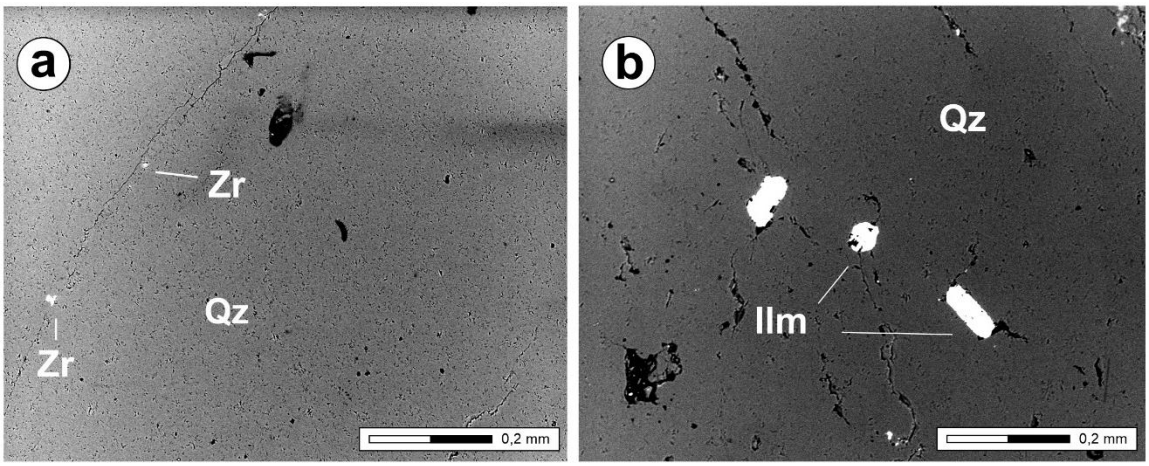


**Source:** Author (2023).

Besides the weak evidence of submicroscopic mineral inclusions, TEM investigations confirmed the presence of two types of inclusions of rutile, shown on Fig. 23. The type I shows rounded shapes, averaging ~10 nm in diameter. The type II is composed of rutile needles, in the blue quartz measure ~0.2 to 0.7 μm. According to Zolensky *et al*. (1988), the type II is too large to produce the blue coloration by Rayleight scattering, therefore, the type I is probably the responsible to collaborate to the light scattering phenomenon, described as the cause of the blue coloration (see Seifert *et al*., 2011).

**Figura 13 -** Inclusions observed by TEM. (a) Needle like inclusions and (b) rounded inclusions observed in quartz crystals from metavolcanic rocks of Rio dos Remédios Group.

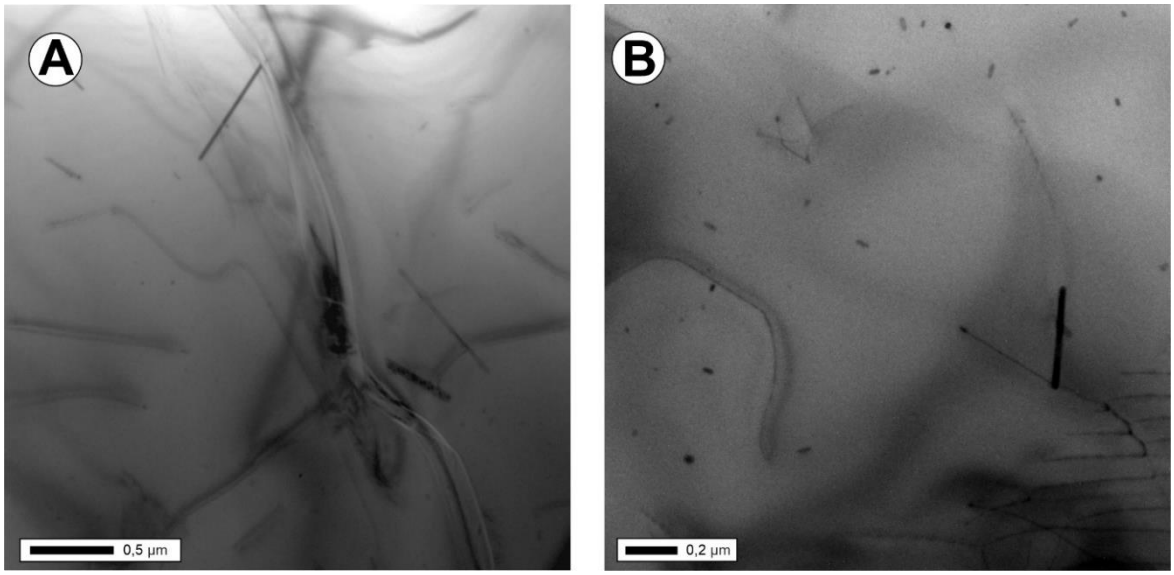


**Source:** Author (2023).

## 5 DISCUSSION

### *Origin of the blue coloration*

The majority of colored quartz varieties is usually associated with transition metal electronic defect structures (Nassau, 1983; Lehmann, 1978). Blue quartz, however, does not show any unusual or particular feature not present is the common milky and colorless quartz. It is currently accepted that the color might be the result of two main mechanisms: (i) the presence of bluish mineral inclusions within the quartz crystals, such as dumortierite, aerinite and magnesium-ribeckite; and (ii) the light scattering process (Rayleigh Scattering) by tiny inclusions inside the quartz crystal (Zolensky *et al.*, 1988; Seifert *et al*., 2011; Iddings, 1904; Pantia *et al*., 2019).The light scattering phenomena, described by the Rayleigh formula, occurs when the particle size is smaller than the wavelength of the light.

Rayleigh scattering relates the intensity of scattered radiation and the frequency of incident radiation (Rocha *et al*., 2010). It occurs when electromagnetic waves interact with particles much smaller than the length of light (Tempfli *et al.*, 2009). The small size of the inclusions is capable of selectively scattering visible light of shorter wavelengths (Wise, 1981).

Rayleigh's formula describes the scattering of light by spherical particles such as dust particles and oxygen and nitrogen molecules. But further studies have shown that non-spherical particles, such as needles, sheet or ribbon-shape minerals satisfy the phenomena requirement (Dörfler, 2002; Seifert *et al*., 2011).

The critical particle size capable of scattering the light and producing the color is still in disagreement in the literature, the common size is described between <55 nm and <27 nm (Dörfler, 2002). Nassau (1983), however, considered particles up to <300 nm in size.

Therefore, the color depends on the size, but not on the nature of the inclusions. Shorter wavelengths (blue) are more effectively scattered than longer wavelengths (red), so the smaller the inclusion dimension, and the greater the spatial density, more vivid the blue hue (Ross, 1941; Pantia *et al*., 2019; Dietrich, 1971; Wise, 1981).

The results observed in Rio dos Remédios metavolcanic rocks revealed the presence of two types of Ti-mineral inclusions. The rounded type I, make up most of the inclusions that satisfy the Rayleigh formula, thus, are more likely to produce the blue coloration. The type two shows a large size range and in some cases are overall too large to satisfy the Rayleigh formula.

According to Zolensky *et al*. (1988), the intensity of the blue coloration varies directly with the density of the inclusions. Only a small number of particles are necessary to produce the color in quartz, also, the presence of large inclusions also cause considerable absorption of the light, consequently the crystal may show various shades from blue to gray.

In the studied samples it was not possible to analyze the concentration of the inclusions, but due their very similar characteristic to the Llano rhyolites, it is assumed that the core and rim show different inclusion concentrations, ensuring the zoning observed (Fig. 8). Besides the apparently high concentration of Ti-mineral inclusions, their size and shape are too small to be present in the regular measurement procedure in this study.

***Origin of the inclusions***

According to the gemological definition, inclusions are any irregularities, foreign body or defect that is inside the mineral (Correa, 2011). For blue quartz crystals there is no consensus as to the nature of the inclusions. During quartz growth, three dimensional defects (inclusions) of fluids or paragenetic minerals (or exsolutions) can be included in its interior (Götze, 2009). The main mechanisms that may condition the formation of inclusions in blue quartz: (1) exsolution; (2) syngenetic to quartz formation and (3) capture of pre-existing minerals during quartz growth (Seifert *et al.*, 2011).

The exsolution mechanism is the most used to justify the origin of rutile in quartz. In this process there is the separation of crystalline phases from a homogeneous solid solution of a mineral. When thermodynamic conditions change, reactions occur and appear as textures of mineral intergrowth (Winge, 2018). The second mechanism implies that the inclusions and the quartz crystallize simultaneously, and for that, the inclusions must crystallize between the center of the crystal and its edges. The third mechanism is more relevant for larger inclusions, which make up magma prior to quartz crystallization. This entrapment model is supported by trace element partitioning and thermometry (Zolensky *et al*., 1988; Seifert *et al.,* 2009; 2011).

The formation of inclusions in quartz is strongly associated with its dimensions. Submicrometer-sized inclusions usually form simultaneously with the quartz crystal and may show growth orientations, while nanoinclusions form by exsolution during cooling (Seifert *et al.,* 2011). Exsolution is the most used model to explain the origin of rutile in quartz (see Frondel, 1962; Meinhold, 2010). The TEM observations were not enough to confirm the density of the inclusions in different parts of the crystal, but the color zoning pattern may indicate a gradient initial Ti concentration, which represents a decrease of temperature during the crystal growth and an origin by exsolution.

According to Seifert *et al*. (2011) and Zolensky *et al*. (1988), the genesis of blue quartz is closely associated with felsic magmas enriched in Ti (100-300 ppm), with crystallization under temperatures between 700-900°C and high pressure. Paramirim metavolcanics exhibit mineralogical, textural, and chemical composition characteristics very similar to other blue quartz occurrences, also the ETRL enrichment in relation to the ETRP and the negative Eu anomaly are compatible with the patterns presented for A-type granites from the Amazonian Craton, which also present the occurrence of blue quartz crystals (see Oga, 1997; Craveiro *et al*., 2019; Dall'Agnol *et al.* 2005; Silva, 2021).

## 6 CONCLUSIONS

Spectroscopy, trace element and TEM analysis carried out in samples of the Rio dos Remédios metavolcanic rocks helped to increase the understanding of this variety of quartz, however, despite the large number of occurrences and the apparently simplicity of quartz composition, the understanding of blue quartz proves to be a challenge. The discussion of the multi-analytical analysis results shown key features that distinguish it from the other varieties:

1. The blue quartz crystals from RR contain abundant nano inclusions of Ti-like minerals, probably rutile, which is considered as result of solid-state exsolution.

2. The typical size of the inclusions, in one or two dimensions (thickness of the rounded type or the cross sections of the needle like inclusions) satisfy the requirements of the Rayleigh formula, that results in wavelength-selective scattering, and contributes to the blue color in the crystals.
3. The presence of the innumerous inclusions is not fully understood but is probably related to special growth conditions, since blue quartz are present as early crystallizing phenocrysts.
4. Blue quartz host rocks are typically rich in Ti and present a high temperature of crystallization (>700°C), which is true for the Brazilian occurrence present in this study. Even so, further research is required to clarify this preferential production in this type of magma composition and if the occurrences show any partner and global geological significance.

# 4 CONCLUSÕES

Os metarriolitos da Formação Novo Horizonte, parte basal do Grupo Rio dos Remédios, caracterizam-se pela textura porfirítica, marcada por fenocristais de feldspato alcalino e quartzo azul. A matriz da rocha é de coloração variável, entre o acinzentado e o marrom. O Seu conjunto mineral característico formado por fenocristais de quartzo azul e K-feldspato, além de cristais de biotita, moscovita, zircão, ilmenita, alanita e rutilo, imersos em uma matriz de mineralogia semelhante.

A assembleia mineral exibe características de alteração hidrotermal deformacional e associada. Os processos hidrotermais são marcados pela substituição total ou parcial de algumas fases minerais, formando minerais secundários, representados principalmente por clorita, sericita, fengita e carbonato. As diferenças composicionais dos tipos de biotita e a presença de alanita também são grandes indícios da ação dos fluidos.

O efeito deformacional é bem-marcado macroscopicamente e microscopicamente marcado pelo contato da foliação da matriz contra os fenocristais, ao invés da deflexão ao redor deles, característica comum devido a presença de megacristais e agregados minerálicos de granulação fina na matriz. Tais feições de alteração se concentram na área de estudo, uma vez que a porção leste do corpo foi mais afetada, formando as fases granada e cianita (Santos et al., 2019). Portanto, a região de Paramirim concentra exemplares que melhor representam as feições primárias do Rio dos Remédios.

A feição principal destas rochas, o quarto azul, se apresentam como cristais euédricos a subédricos, por vezes, se apresentam bipiramidados e altamente fraturados, com dimensões entre 3 e 6 mm, formando agregados na matriz da rocha. Em sua maioria, os fenocristais exibem um zoneamento entre centro e borda dos cristais, que variam em tons de azul. Em certas posições cristalográficas, os cristais mais fraturados exibem um reflexo azul-esbranquiçado (iridescência) em suas bordas.

A formação de cristais de quartzo azul está frequentemente associada a presença de inclusões submilimétricas no interior dos cristais, cujas dimensões sejam concordantes com àquelas concordantes com a fórmula de Rayleigh, causando o espelhamento da luz e geração da cor. Os cristais das rochas metavulcânicas analisadas contêm abundantes nanoinclusões de minerais semelhantes ao Ti, provavelmente rutilo. O tamanho típico das inclusões, em uma ou duas dimensões (espessura do tipo arredondado ou as seções transversais da necessidade como inclusões) satisfazem os requisitos da fórmula de Rayleigh, que resulta em espelhamento seletivo de comprimento de onda e contribui para a cor azul nos cristais.

A presença das inúmeras inclusões não é totalmente compreendida, mas provavelmente está relacionada a condições especiais de crescimento, como resultado da exsolução do estado sólido, uma vez que o quartzo azul está presente como fenocristais de cristalização precoce.

As rochas portadoras de quartzo azul são tipicamente ricas em Ti e apresentam alta temperatura de cristalização (>700°C), alta sílica e caráter peraluminosos, com afinidades magmáticas transicionais e assinaturas do tipo A derivadas da crosta intraplaca. Todas estas características estão presentes na ocorrência apresentada neste estudo, no entanto mais pesquisas são necessárias para esclarecer esta produção preferencial neste tipo de composição de magma e se as ocorrências mostram algum parceiro e significado geológico global.

# REFERÊNCIAS

ABDEL-RAHMAN, A. F. M. Nature of biotites from alkaline, calc-alkaline, and peraluminous magmas. Journal of Petrology, 35(2):525-541, 1994.https://doi.org/10.1093/petrology/35.2.525

ALKMIM, F. F., BRITO NEVES, B. B., ALVES, J. A. C. Arcabouço tectônico do Cráton do São Francisco – uma revisão. In: Dominguez J.M., Misi A. (eds.). O cráton do São Francisco. Reunião preparatória do II Simpósio sobre o cráton do São Francisco. Salvador: SBG/Núcleo BA/SE/SGM/CNPq. p.45-62, 1993.

ALKMIM, F. F., PEDROSA-SOARES, A. C., NOCE, C. M., CRUZ, S. C. P. Sobre a evolução tectônica do Orógeno Araçuaí-Congo Ocidental. Geonomos,15(1):25-43, 2007. https://doi.org/10.18285/geonomos.v15i1.105

ALMEIDA, F. F. M. O Cráton do São Francisco. Revista Brasileira de Geociências, 7(4):349-364, 1977.

ARCANJO, J. B. A., VARELA, P. H. L., MARTINS, A. A. M., LOUREIRO, H. S. C., NEVES, J. P. (Eds.). Projeto Vale do Paramirim: Estado da Bahia. Programa Levantamentos Geológicos Básicos do Brasil -PLGB. Convênio CBPM/CPRM. Escala 1:200.000. Relatório interno. Salvador: CPRM Bahia, 1999.

BABINSKI, M., BRITO NEVES, B. B., MACHADO, N., NOCE, C. M., UHLEIN, A., VANSCHMUS, W. R. Problemas da metodologia U/Pb em zircões de vulcânicas continentais: caso do Grupo Rio dos Remédios, Supergrupo Espinhaço, no Estado da Bahia. In: 42° Congresso Brasileiro de Geologia,42., 1994. Anais... Sociedade Brasileira de Geologia, Balneário Camboriú, 2:409-410, 1994.

BARBOSA, J. S. F. Geologia da Bahia: pesquisa e atualização. Salvador: CBPM, p. 33-85.2v. (Série de publicações especiais; 13), 2012.

BARBOSA, J. S. F., SABATÉ, P. Colagem Paleoproterozóica de Placas Arqueanas do Cráton do São Francisco na Bahia. Revista Brasileira de Geociências, 33(1):714, 2003.

BARKER, D. S., BURMESTER, R. F. Leaching of quartz from precambrian hypabyssal rhyolite porphyry, Llano County, Texas. Contributions to Mineralogy and Petrology, 28(1):1-8, 1970. https://doi.org/10.1007/BF00389222.

BETSI, T. B., LENTZ, D. R. The nature of "quartz eyes" hosted by dykes associated with Au-Bi-As-Cu, Mo-Cu, and base-metal-Au-Ag mineral occurrences in the mountain freegold region (Dawson Range), Yukon, Canada. Journal of Geosciences,55(4):347-368, 2010.https://doi.org/10.3190/jgeosci.082.

BRADLEY, J. Geology of the West Coast Range, part III: Porphyroid metassomatism. Papers and Proceesings of the Royal Society of Tasmania,91:163-190, 1957.

BRITO NEVES, B. B., FUCK, R. A., PIMENTEL, M. M. A colagem Brasiliana na América do Sul: uma revisão. Brazilian Journal of Geology,44(3):493-518, 2014.https://doi.org/10.5327/Z2317-4889201400030010.

CARLIN, A. C., ZANARDO, A., NAVARRO, G. R. B. Caracterização petrográfica das rochas encaixantes da mineralização aurífera do Depósito Lavra Velha –região de Ibitiara, borda oeste da Chapada Diamantina, Bahia. Geociências Unesp, 37(2):253-265, 2018.https://doi.org/10.5016/geociencias.v37i2.12113.

CAVALCANTI, J. C. C., MOREIRA, M. D., OLIVEIRA, W. D., SIQUEIRA, A. P., SILVA, B. C. E., CUNHA, J. C., MONTEIRO, M. D., OLIVEIRA, N. D., ARAÚJO, N. B., FRÓES, R. J. B., SOUZA, S. L. Projeto prospecção de cassiterita na Chapada Diamantina-BA. Companhia Baiana de Produção Mineral, 123 p, 1980.

CAXITO, F. A., SANTOS, L. C. M. L., GANADE DE ARAÚJO, C. E., BENDAOUD, A., FETTOUS, E. H., BOUYO HOUKETCHANG, N. Toward an integrated model of geological Evolution for NE Brazil-NW Africa: The Borborema Province and its connections to the Trans-Saharan (Benino-Nigerian and Tuareg shields) and Central African orogens. Brazilian Journal of Geology,50(2):1-38, 2020. https://doi.org/10.1590/2317-4889202020190122

CORREA, M. Variedades gemológicas de quartzo na Bahia, geologia, mineralogia, causas de cor e técnicas de tratamento. Dissertação (Mestrado) – Programa de Pós-graduação em mineralogia e petrologia, Universidade de São Paulo, 2011.

COX, K. G., BELL, J. D., PANKHURST, R. J. The Interpretation of Igneous Rocks. London: George Allen and Unwin, 450 p, 1979.
17

CRAVEIRO, G. S., XAVIER, R. P., VILLAS, R. N. N. The Cristalino IOCG deposit: an example of multi-stage events of hydrothermal alteration and copper mineralization. Brazilian Journal of Geology, 49(1), 2019: DOI: 10.1590/2317-488920192018001

CRUZ DA SILVA, D., LIRA SANTOS, L., QUEIROGA, G., LIRA SANTOS, G., TEDESCHI, M. Multi-method characterization of rare blue quartz-bearing metavolcanic rocks of the Rio dos Remédios Group, Paramirim Aulacogen, NE, Brazil. Brazilian Journal of Geology. (Prelo), 2023.

CRUZ, S. C. P., ALKMIM, F. F. The Paramirim Aulacogen. In: Heilbron, M., Cordani, U.G., Alkmim F.F. (Eds.). São Francisco Craton, Eastern Brazil. Springer, 1:97-115, 2017. https://doi.org/10.1007/978-3-319-01715-0

CRUZ, S. C. P., DIAS, V. M., ALKMIM, F. F. A interação tectônica embasamento/cobertura em aulacógenos invertidos: um exemplo da Chapada Diamantina Ocidental. Revista Brasileira de Geociências, 37(4):111-127, 2007.

DALL'AGNOL, R., TEIXEIRA, N. P., RÄMÖ, O. T., MOURA, C. A. V., MACAMBIRA, M. J. B., OLIVEIRA, D. C. Petrogenesis of the Paleoproterozoic, rapakivi, A-type granites ofthe Archean Carajás Metallogenic Province, Brazil. Lithos, 80(1):101-129, 2005.

DANDERFER FILHO, A., DARDENNE, M. A. Tectonoestratigrafia da bacia Espinhaço na porção centro-norte do Cráton do São Francisco: registro de uma evolução poliistórica descontínua. Revista Brasileira de Geociências,32(4):449-460, 2002.

DANDERFER FILHO, A. Geologia Sedimentar e Evolução Tectônica do Espinhaço Setentrional, Estado da Bahia. PhD Thesis, Universidade de Brasília, Brasília, DF, Brasil, 2000.

DANDERFER FILHO, A., LANA, C. C. NALINI JÚNIOR, H. A., COSTA, A. F. O. Constraints on the Statherian evolution of the intraplate rifting in a Paleo-Mesoproterozoic paleocontinent: New stratigraphic and geochronology record from the eastern São Francisco craton. Gondwana Research, 28(2):668-688, 2014.https://doi.org/10.1016/j.gr.2014.06.012

DEER, W.A., HOWIE, R.A., ZUSSMAN, J. An introduction to the rock-forming minerals. Harlow: Longman Scientific and Technical, 1992.
DIETRICH, R. V. Quartz-two new blues: Mineralogical Record, 2: 79-82, 1971.

DÖRFLER, H.D. Grenzflächen und colloid-disperse Systeme. Berlin: Springer, 989 p, 2002.

DUMAS, A. O Conde de Monte Cristo. Paris: P. Baudry, 1844.

ETHERIDGE, A., VERNON, R., H. A deformed polymictic conglomerate -the influence of grain size and composition on the mechanism and rate of deformation. Tectonophysics, 79(3-4):237-254, 1981. https://doi.org/10.1016/0040-1951(81)90115-3.

FREZZOTTI, M. L, TECCE, F., CASAGLI, A. Raman spectroscopy for fluid inclusion analysis, Journal of Geochemical Exploration, 112: 1-20, ISSN 0375-6742, 2012. DOI: https://doi.org/10.1016/j.gexplo.2011.09.009.

FRONDEL, C. The System of Mineralogy of James Dwight Dana and Edward Salisbury Dana. 3(7), Silica Minerals. John Wiley and Sons, New York, 334 p, 1962.

GAO, P., GARCIA-ARIAS, M., CHEN, Y. X., ZHAO, Z. F. Origin of peraluminous A-type granites from appropriate sources at moderate to low pressures and high temperatures. Lithos, 352-353: 105287, 2020.https://doi.org/10.1016/j.lithos.2019.105287

GÖTZE J. Chemistry, textures and physical properties of quartz geological interpretation and technical application. Mineralogical Magazine, 73:645-671, 2009.

GROS, K., SLABY, E., JOKUBAUSKAS, P., SLÁMA, J., KOZUB-BUDZYN. Allanite geochemical response to hydrothermal alteration by alkaline, low-temperature fluids. Minerals, 10(5):392-422, 2020.https://doi.org/10.3390/min10050392

GUADAGNIN, F., CHEMALE JR, F. Detrital zircon record of the Paleoproterozoic to Mesoproterozoic cratonic basins in the São Francisco Craton. Journal of South American Earth Sciences, 60:104-116, 2015. https://doi.org/10.1016/j.jsames.2015.02.00718

GUIDOTTIC, V. Compositional variations of muscovite as a function of metamorphic grade and assemblage in metapelites from N.W. Maine. Contributions to Mineralogy and Petrology, 41:33-42, 1987.

GUILLOPE, M., POIRIER, J. P. Dynamic recrystallization during creep of single-crystalline halite: an experimental study. Journal ofGeophysicalResearch,84(B10):5557-5567, 1979.https://doi.org/10.1029/JB084iB10p05557

GUIMARÃES, J. T., ALKMIM, F. F., CRUZ, S. C. P. Supergrupos Espinhaço e São Francisco. In: Barbosa J.S.F., Mascarenhas J., Domingues J.M.L., Correa-Gomes L.C. Geologia da Bahia: pesquisa e atualização de dados. Salvador: CBPM, 2012.

GUIMARÃES, J. T., MARTINS, A. A. M., ANDRADE FILHO, E. L., LOUREIRO, H. S. C., ARCANJO, J. B. A., ABRAM, M. B., SILVA, M. G., BENTO, R. V. Projeto Ibitiara-Rio de Contas. Série Arquivos Abertos; 31. Salvador: CPRM-Bahia, 70 p, 2008.

GUIMARÃES, J. T., MARTINS, A. A. M., LOUREIRO, H. S. C., ARCANJO, J. B. A., NEVES, J. P., ABRAM, M. B., SILVA, M. G., MELO, R. C., BENTO, R. V. Projeto Ibitiara -Rio de Contas. Salvador: CPRM/CBPM, Programa Recursos Minerais do Brasil,182 p, 2005.

GUZZO, P. L., BARRETO, S. B., MIRANDA, M. R. Gamma-rays and heat-treatment conversions of point defects in massive rose quartz from the Borborema Pegmatite Province, Northeast Brazil. Phys Chem Minerals 44:701–715, 2017. DOI: https://doi.org/10.1007/s00269-017-0895-0.

HALDER, M., PAUL, D., SENSARMA, S. Rhyolites in continental mafic large igneous provinces: petrology, geochemistry and petrogenesis. GeoscienceFrontiers,12(1):53-80, 2021. https://doi.org/10.1016/j.gsf.2020.06.011.

HEILBRON, M., CORDANI, U. G., ALKMIM, F. F. São Francisco Craton, eastern Brazil: tectonic genealogy of a miniature continent. New York: Regional Geology Reviews, Springer Berlin Heidelberg,331 p, 2017. https://doi.org/10.1007/978-3-319-01715-0.

HEINRICH, P. V. Llanite and the Blue Quartz of Texas. The Backbender's Gazette, 45(5):5-12, 2014.

IDDINGS, J. P. Quartz-feldspar-porphyry (graniphyroliparose-alaskose) from Llano, Texas. Journal of Geology, 12(3):225-231, 1904. https://doi.org/10.1086/621145

HEMMATI, A., GHAFOORI, M., MOOMIVAND, H., LASHKARIPOUR, G. R. The effect of mineralogy and textural characteristics on the strength of crystalline igneous rocks using image-based textural quantification, Engineering Geology, 266:105467, 2020, ISSN 0013-7952. DOI: https://doi.org/10.1016/j.enggeo.2019.105467.

KATS, A. Hydrogen in α-quartz. Philips Res Repts, 17:113–195 (201–279), 1962.

LEHMANN, G. Farben von Mineralien und ihre Ursachen. Fortschritte der Mineralogie, 56:172-252, 1978.

LOUREIRO, H. S. C., GUIMARÃES, J. T., MARTINS, A. A. M., ANDRADE, E. L., ARCANJO, J. B. A., NEVE, J. P., ABRAM, M. B., SILVA, M. G., MELO, R. C. Projeto Barra-Oliveira dos Brejinhos, Estado da Bahia. Salvador: Companhia Brasileira de Pesquisa Mineral e CPRM, 156 p, 2008.

MEDEIROS, K. O. P. Estratigrafia de Sequências do Supergrupo Espinhaço na Região Entre Macaúbas e Canatiba –Bahia. MS Dissertation, Instituto de Geociências, Universidade Federal da Bahia, Salvador, 2013.

MEINHOLD, G. Rutile and its applications in the earth sciences. Earth-Science Reviews, 102:128, 2010.

NACHIT, H., IBHI, A., ABIA, E. H., OHOUD, M. B. Discrimination between Primary Magmatic Biotites, Reequilibrated Biotites and Neoformed Biotites. Comptes Rendus Geoscience, 337(16):1415-1420, 2005.https://doi.org/10.1016/j.crte.2005.09.002

NASSAU, K. The Physics and Chemistry of Color. Wiley, New York, 2, 496p, 1983.

OGA, D. P. Estudo químico mineralógico e importância das ocorrências de Sn-In das metavulcânicas da região de Paramirim-Ba. MS Dissertation, Instituto de Geociências, Universidade de Brasília, Brasília, 1997.

PANTIA, A. I., CRUZ DA SILVA, D., FILIUȚĂ, A. Blue quartz in Brasil: the Rio dos Remédios occurence-preliminary study. Pesquisa em Geociências, 49(1), 2022.

PANTIA, A. I., FILIUȚĂ, A., LŐRINCZ, S. Blue quartz around the globe. Muzeul Olteniei Craiova. Oltenia. Studii şi comunicări. Ştiinţele Naturii,35(2), 2019.

ROCHA, M. N., FUJIMOTO, T. G., AZEVEDO, R. S., MURAMATSU, M. O azul do céu e o vermelho do pôr-do-sol. Revista Brasileira De Ensino De Física, 32(3):1-3, 2010. DOI: https://doi.org/10.1590/S1806-11172010000300013.

ROSA, M. L. S. Geologia, geocronologia, mineralogia, litogeoquímica e petrologia do Batólito Monzo-Sienítico Guanambi-Urandi (SW-Bahia). PhD Thesis, Universidade Federal da Bahia, Salvador, 1998.

SANTANA, A. V. A. Análise estratigráfica em alta resolução: exemplo em rampa carbonática dominada por microbialitos da Formação Salitre, Bacia do Irecê, Bahia. PhD Thesis, Universidade de Brasília, Brasília, 2016.

SANTOS, J. M. A., MACHADO, A., LENZ, C., LIZ, L. C. C., COSTA, I. A. A. Geologia, petrografia e geoquímica das rochas metavulcânicas ácidas da Estrada Real, Rio de Contas (BA). Pesquisas em Geociências, 46(2):e699, 2019.https://doi.org/10.22456/1807-9806.95462

SANTOS, L. C. M. L., SANTOS, E. J., DANTAS, E. L., LIMA, H. M. Análise estrutural e metamórfica da região de Sucuru (Paraíba): implicações sobre a evolução do Terreno Alto Moxotó, Província Borborema. Geologia USP. Série Científica, 12(3):5-20, 2012. https://doi.org/10.5327/Z1519-874X2012000300001

SCHOBBENHAUS, C. As tafrogêneses superpostas Espinhaço e Santo Onofre, Estado da Bahia: Revisão e novas propostas. Revista Brasileira de Geociências, 26(4):265-276, 1996.

SCHOBBENHAUS, C., HOPPE, A., BAUMANN, A. Idade U/Pb do vulcanismo Rio dos Remédios, Chapada Diamantina, Bahia. In: Congresso Brasileiro de Geologia, Balneário Camboriú, 38., 1994. Boletim de Resumos Expandidos,2:397-398, 1994.

SCHOBBENHAUS, C., KAUL, P. F. T. 1971. Contribuição à estratigrafia da Chapada Diamantina Bahia Central. Mineração e Metalurgia, 53:116-120, 1971.

SEIFERT, W., RHEDE, D., THOMAS, R., FÖRSTER, H. J., LUCASSEN, F., DULSKI, P., WIRTH R. Distinctive properties of rock-forming blue quartz: inferences from a multi-analytical study of submicron mineral inclusions. Mineralogical Magazine,75(4):2519-2534, 2011.https://doi.org/10.1180/minmag.2011.075.4.2519

SEIFERT, W., RHEDE, D., FÖRSTER, H.-J., THOMAS, R. Accessory minerals as fingerprints for the thermal history and geochronology of the Caledonian Rumburk granite. Neues Jahrbuch für Mineralogie, Abhandlungen, 186:215-233, 2009.

SILVA, F. F., OLIVEIRA, D. C., ANTONIO, P. Y. J., D'AGRELLA FILHO, M. S., LAMARÃO, C. N. Bimodal magmatism of the Tucumã area, Carajás province: U-Pb geochronology, classification and processes. Journal of South American Earth Sciences, 72:95-114, 2016. https://doi.org/10.1016/j.jsames.2016.07.016.

TEIXEIRA, L. R. Projeto Ibitiara-Rio de Contas: relatório temático de litogeoquímica. Programa Levantamentos Geológicos Básicos do Brasil. Relatório interno. Salvador: CPRM, 33 p, 2005.

TEMPFLI, K., HUURNEMAN, G., BAKKER, W., JANSSEN, L., BAKKER, W., FERINGA, W., GIESKE, A., GRABMAIER, K., HECKER, C., HORN, J. Principles of Remote Sensing: An Introductory Textbook. 4th Edition, ITC, Enschede, 2009.

VERNON, R. H. Evaluation of the 'quartz-eye' hypothesis. Economic Geology,81(6), 1986:1520-1527.https://doi.org/10.2113/gsecongeo.81.6.1520.

VERNON, R. H. K-feldspar augen in felsic gneisses and mylonites—deformed phenocrysts or porphyroblasts? Geologiska Föreningen i Stockholm Förhandlingar,112(2), 1990:157-167.https://doi.org/10.1080/11035899009453175.

WEIS, Z. A procedure for classifying rock-forming chlorites based on microprobe data. Rendiconti Lincei, 9:51-56, 1998. https://doi.org/10.1007/BF02904455.

WISE, M. A. Blue quartz in Virginia. Virginia Minerals. Virginia Division of Mineral Resources, Charlottesville, 27(2):9-12, 1981.

WILLIAMS, M. L., BURR, J. L. Preservation of quartz phenocrysts and kinematic indicators in metamorphosed and deformed Proterozoic rhyolites, southwestern North America. Journal of Structural Geology,22:139, 1990.

WINKLER, H. G. F., SCHULTES, H. On the problem of alkali feldspar phenocrysts in granitic rocks. Neues Jahrbuch für Mineralogy, 12:558-564, 1982.

WRIGHT, T. L., STEWART, D. B. X-ray and optical study of alkali feldspar: I. Determination of composition and structural state from refined unit-cell parameters and 2V. AmericanMineralogist,53(1-2):38-87, 1968.

WU, D. J. P., FEI XIA, G. H., JING, L. The mineral chemistry of chlorites and its relationship with uranium mineralization from Huangsha uranium mining area in the middle Nanling Range, SE China. Minerals, 9(3):199, 2019. https://doi.org/10.3390/min9030199.

ZHANG. H. F, ZHANG. L., HARRIS. N., JIN. L. L., YUAN. H.L. U-Pb zircon ages, geochemical and isotopic compositions of granitoids in Songpan-Garze fold belt, eastern Tibetan Plateau: constraints on petrogenesis and tectonic evolution of the basement. Contributions to Mineralogy and Petrology, 152(1):75-88. 2006. https://doi.org/10.1007/s00410-006-0095-2

ZHANG, W., LENTZ, D.R., THORNE, K.G., MCFARLANE, C. Geochemical characteristics of biotite from felsic intrusive rocks around the Sisson Brook W-Mo–Cu deposit, west–central New Brunswick: an indicator of halogen and oxygen fugacity of magmatic systems. Ore GeologyReview,77:82-96, 2016. https://doi.org/10.1016/j.oregeorev.2016.02.004

ZHANG, Z. S., HUA, R. M., JI, J. F., ZHANG, Y. C., GUO, G. L., YIN, Z. P. Characteristics and formation conditions of chlorite in N°. 201 and N°. 361 uranium deposits. Acta Mineralogy, 27:161-172, 2007.

ZOLENSKY, M. E., SYLVESTER, P. J., PACES, J. B. Origin and significance of blue coloration in quartz from Llano rhyolite (llanite), north-central Lllano County, Texas. American Mineralogist, 73:313-332, 1988.